12-14-2011

Background-Oriented Schlieren Pattern Optimization

Jeffery E. Hartberger

BACKGROUND-ORIENTED SCHLIEREN PATTERN OPTIMIZATION

THESIS

Jeffery E. Hartberger, Captain, USAF

AFIT/GAE/ENY/11-D16

DEPARTMENT OF THE AIR FORCE
AIR UNIVERSITY

AIR FORCE INSTITUTE OF TECHNOLOGY

Wright-Patterson Air Force Base, Ohio

AFIT/GAE/ENY/11-D16

BACKGROUND-ORIENTED SCHLIEREN PATTERN OPTIMIZATION

THESIS

Presented to the Faculty

Department of Aeronautics and Astronautics

Graduate School of Engineering and Management

Air Force Institute of Technology

Air University

Air Education and Training Command

In Partial Fulfillment of the Requirements for the

Degree of Master of Science in Aeronautical Engineering

Jeffery E. Hartberger, B.S.A.E.

Captain, USAF

December 2011

AFIT/GAE/ENY/11-D16

BACKGROUND-ORIENTED SCHLIEREN PATTERN OPTIMIZATION

Jeffery E. Hartberger, B.S.A.E.
Captain, USAF

Approved:

Mark F. Reeder, PhD (Chairman)	Date
Donald L. Kunz, PhD (Member)	Date
Capt James L. Rutledge, PhD (Member)	Date

Abstract

This paper describes a test series to investigate background patterns used for the Background-Oriented Schlieren (BOS) field density measurement technique. Several varying background patterns were substituted under similar fluid density conditions to visualize and isolate the effects of patterns in the background images. A qualitative comparison was completed of the flow visualization results of each background pattern to categorize background conditions that improved the flow visualization image. Changes in background patterns revealed significant changes in flow visualization. Pattern contrast, spacing and sizing all played large parts in the quality of the visual density gradient imaging during the BOS test series.

Acknowledgements

I would like to thank my advisers Dr. Reeder and Dr. Kunz for their support throughout this research project, and Carrie Reinholtz, Kenneth Scott and Dr. Wehrmeyer for their support in the execution of the testing at Arnold Air Force Base (AFB) to complete this project. I would also like to thank my family for their unwavering support throughout my career.

Jeffery E. Hartberger

Table of Contents

List of Figures

List of Tables

List of Symbols

List of Abbreviations

BACKGROUND-ORIENTED SCHLIEREN PATTERN OPTIMIZATION

I. Introduction

1.1 Background

BOS is a derivative of the classical schlieren technique and has been referred to as synthetic schlieren in the past. BOS has increased in use over the past several years due to the development of processing software and digital optics. Prior to BOS, common methods of imaging density gradients in fluids have been schlieren and shadowgraph photography. Developments in the schlieren and shadowgraph methods can be found in Hargather [4]. These techniques are still used today and they require relatively large visual access to areas of interests within the flow and offer the standard qualitative images of shock waves common among aerodynamic research as seen in Fig. 1.1.

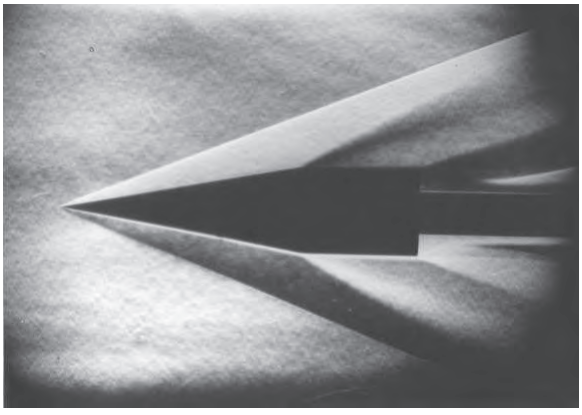

Figure 1.1: Typical schlieren photograph of shock waves

This older method of imaging has drawbacks that include the necessity of large optical ports with expensive optical quality glass and limited fields of view. The BOS technique requires very little optical access to maintain a relatively large field of view. Optical access geometry depends on the field of view of the subject needed and the lighting used during testing. Hargather described the advantage of BOS best when he stated, "BOS is unique in that it requires a limited amount of inexpensive equipment, and in the simplest case can be applied with almost any consumer grade digital camera and a distant background" [4].

The BOS technique of measuring density gradients in fluids has been used increasingly over the last decade, due largely to incremental technology improvements that have reduced the cost of electronics. Improvements in camera imaging, lasers for lighting and computer processing speed have all contributed to the rise of alternate techniques like BOS. Flow visualization techniques that are currently being investigated along with BOS are Particle Image Velocimetery (PIV) and Planar Doppler Velocimetry (PDV), among others. These techniques use lasers to illuminate the fluid and require seeding to visualize the fluid particles. BOS does not require the flow to be seeded for visualization and is capable of collecting more data than schlieren, to include three dimensional flow data. Research is also being done to apply BOS to three dimensional field flow visualization as reported by Goldhahn [2]. Many of the other techniques being researched, such as PIV and PDV, require more expensive equipment such as lasers. High strength lighting such as lasers are used to illuminate the seeded flow at short durations to facilitate small camera exposure times. Tests

with BOS use laser lighting at times, but it is not always necessary. The lighting source requirement is driven by the test setup. The distance between the background and the camera, the access space available for viewing and the speed of flow being imaged are typical driving factors for the lighting source. A long distance between the background and camera may require a strong lighting source to sufficiently illuminate the background. The optical access area of a test setup may be very small and only allow for a small focused light source. Finally, lighting needs can be influenced by the velocity of the flow to be imaged. High speed flow imaging would normally benefit from laser or flash lamp lighting. If high speed flow such as transonic flow is being imaged, then one would normally want very short exposure times to prevent image blur. High speed flow drives rapidly changing density gradients. Rapidly changing density gradients correlate to rapidly changing positions of dot patterns in the background. To properly image the rapidly changing dot patterns with very short exposure times a high intensity short duration light source is necessary. These types of setup requirements could drive the tester toward the use of a laser or flash lamp source for lighting in some cases.

No comprehensive research has been discovered to date that deals specifically with analyzing how changes in background images affect the image quality of the density gradient. Anecdotal discussions in papers such as Richard [8] and Vasudeva [10] use patterns with no detailed explanation of the research methods used to validate the patterns. Pattern use for BOS has extensively been through trial and error and PIV particle size recommendations.

1.2 System Description

The BOS technique is based on analyzing the variations found in the refractive index of a fluid flow. As light passes through a gas with a refractive index gradient, the light is bent in the direction of increasing density [7]. A thorough background of the technique can be found in Richard [8]. Many other new visualization techniques in use today require the flow to be seeded in order to visualize. BOS is able to achieve imaging of the changing density gradients without seeding the flow particles, as described in Hargather [5]. Goldhahn gives a good general description of the BOS technique when he states that it is the time-rate-of-change of the refractive index field [2].

For the BOS technique, high resolution digital cameras are used to capture images of the flow. The first image can be a baseline image of the background without a density gradient present, or air off, and a second image can be taken with a density gradient present, or air on, for comparison. Two successive air on images can also be taken for comparison. Standard PIV software is used to analyze the displacement vectors of the background pattern between images when compared to each other. The deflection angle of the light passing through the density gradient causes a distortion in the background image. The dots in the background image change position due to the light distortion. The PIV software analyzes the displacement vectors of the dots and outputs gray scale images similar to a schlieren photograph [7]. The change in displacement vectors of the dots due to the density gradient can be seen in Fig. 1.2.

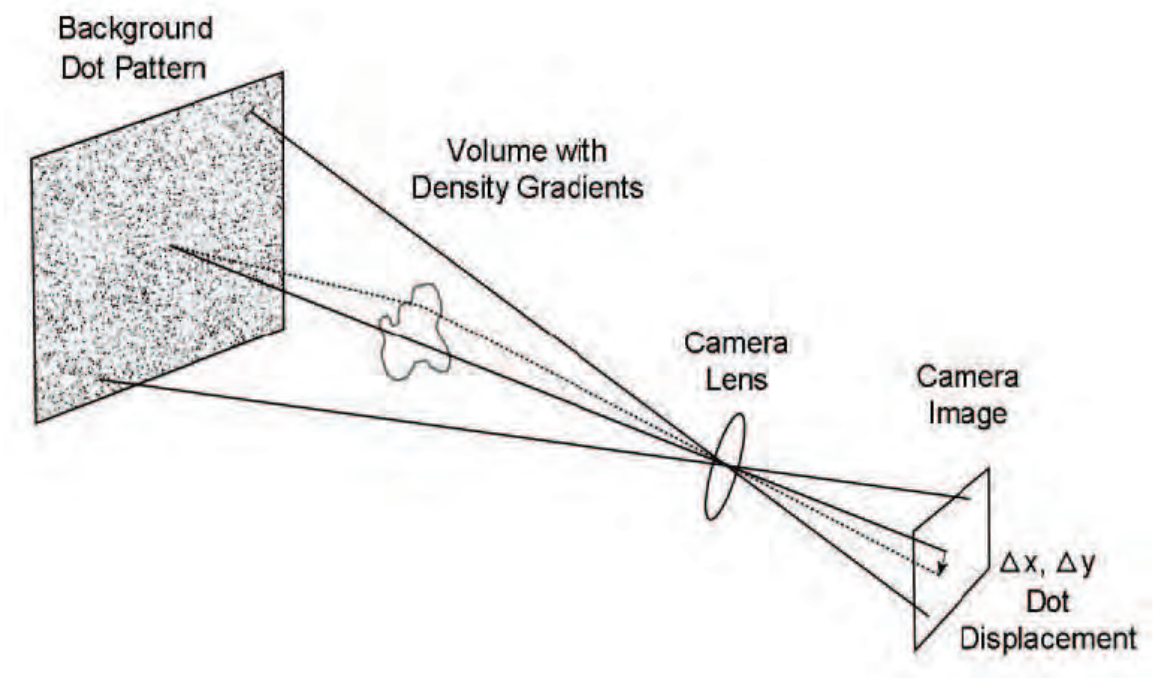

Figure 1.2: Conceptual drawing of BOS imaging through a density gradient [7]

$\triangle x$ and $\triangle y$ are horizontal and vertical displacements respectively of the background dot pattern due to the light waves passing through the density gradient.

BOS is based on the relationship between the refractive index and density gradients as seen in the Gladstone-Dale equation, Eq. 1.1, where n is refractive index, ρ is density ($kg \times m^{-3}$) and $G(\lambda)$ is the Gladstone-Dale number [8].

$$\frac{n-1}{\rho} = G(\lambda) \tag{1.1}$$

Where $G(\lambda)$ is defined by Eq. 1.2:

$$G(\lambda) = 2.2244 \times 10^{-4} \times \left(1 + \left(\frac{6.7132 \times 10^{-8}}{\lambda}\right)^2\right) \tag{1.2}$$

with λ = wavelength (m).

When we decide which λ, or light source, to use in Eq. 1.2 we have to consider optical effects and camera availability. Light with varying wavelengths is less desired due to chromatic abberation effects from optical focusing of multiple wavelengths. Collimated single wavelength light, such as that from a laser, are sometimes preferred, but the choice of the light source to use is also partially dependent on other factors, such as the quantum efficiency of the image sensor in the camera. Light wavelengths in the white range, like the lighting used in this test, often match well to many modern camera sensitivity ranges, and the influence of wavelength on the Gladstone-Dale number, given in Eq. 1.2, is relatively small given the wavelength range for visible light, which is approximately 400-700 nm.

The radius of curvature, r, of the light passing through the density gradient is expressed in Eq. 1.3. This shows the radius of curvature is inversely proportional to the gradient of the refractive index [7].

$$\frac{1}{r} = \nabla(n) \tag{1.3}$$

The BOS images are derived from data through analysis software while standard schlieren images are taken directly from the image of the deflected light rays [9]. The described diffraction zone of the bent light rays can be seen in Fig. 1.3. The schlieren technique images the density gradient by only imaging the light rays that follow a straight path. The curved light rays that are deflected around the density gradient

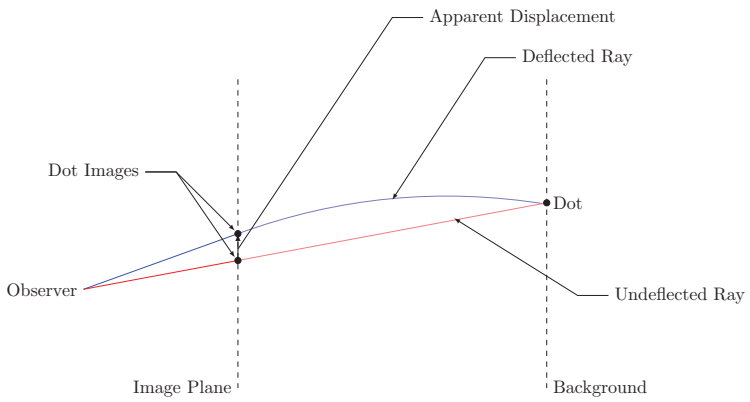

Figure 1.3: Diffraction zone of light rays passing through a density gradient [9]

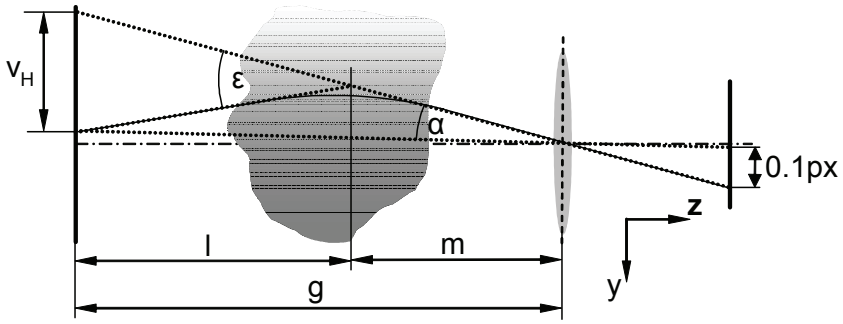

Figure 1.4: Geometry for light diffraction sensitivity [2]

do not get captured by the image sensor and give the image its blurred appearance in density gradient fields. Due to the derived result of BOS, it is prudent to verify BOS images with other flow image methods when new techniques are used.

The sensitivity of BOS imaging is described well in Goldhahn [2]. The deflection angle ε is simplified in Eq. 1.4. Where ν_{px} is the corresponding pixel shift, β is the deviation angle and f is the focal length. Reference Fig. 1.4.

$$\varepsilon \approx \left(1 + \frac{m}{l}\right) \cdot \nu_{px} \left(\frac{g - f}{g \times f}\right) \cdot \cos^2(\beta) \tag{1.4}$$

The deviation angle β is typically very small, therefore $\cos^2(\beta)$ tends to 1 [2]. This indicates that the sensitivity of the deflection angle ε is primarily dependent on lens focal length, position and overall size of density gradient in the test setup and smallest detectable pixel shift ν_{px}. The test setup often defines the geometry of the first three, but the detectable pixel shift is dependent on the background pattern, the image sensor and the processing software.

From PIV recommendations on particle size, the background dot size should be scaled to allow for contrasting objects in the 2 to 4 pixel size range, in order to best capture pixel shift [6, p. 167]. This is shown graphically in Fig. 1.5. Raffel shows in this figure, through evaluation by Monte Carlo simulations, that the lowest uncertainty in cross-correlation of a particle between two images is approximately 2.5 pixels. In general, most BOS literature translates this to a 2 to 4 pixel range as being near ideal. The application of this pixel size rule to specific test cases is done through simple geometry. An example would be how Reinholtz applied this recommendation to work in the Arnold AFB 16 foot transonic wind tunnel test [7]. For this test, the density gradient subject area of interest was $4.5'$ x $4.5'$ square located midway between the camera and background. This translated to a $9'$ x $9'$ square background. A camera with 2048 x 2048 pixel resolution was used. Since the setup and resolution are symmetric, we can take either dimension and divide the background length by available pixels. This is shown in Eq. 1.5, and gives a estimated dot size of approximately 0.16" for this setup. How this recommended particle size was applied to the test in this thesis is discussed in chapter 2.

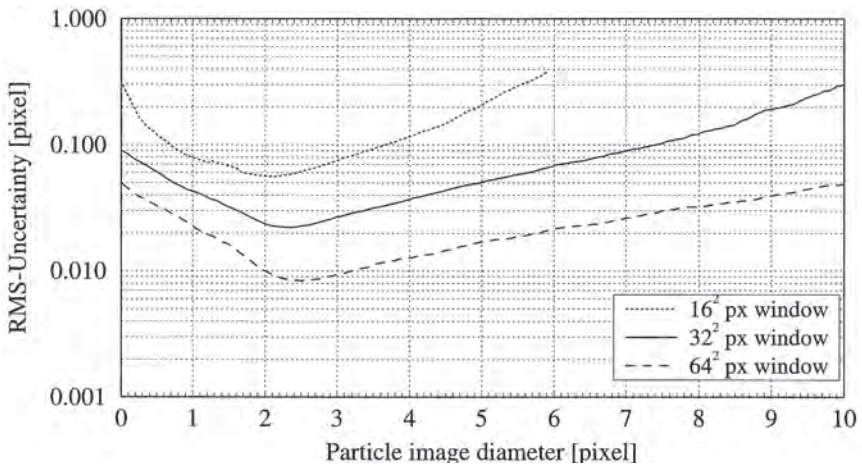

Figure 1.5: Uncertainty versus particle image diameter [6, p. 167]

$$9' = 108" \div 2048\, pixels \approx 0.053\, \frac{inch}{pixel} \times 3\, pixel\, recommendation \approx 0.16" \qquad (1.5)$$

Hargather states the bottom line of BOS sensitivity well when he remarks, "In general, a distant background, imaged with a long focal-length lens by a camera of high pixel resolution, results in the greatest sensitivity" [4]. But this is followed by the comment that the sensitivity is constrained by the depth of field of the lens. The effects of depth of field on image quality is not well known in BOS. My opinion after reading BOS papers and talking to local researchers is that an increased depth of field would contribute to better image sensitivity. I believe that image quality is affected by the ability of the lens to focus on the background pattern while still managing some amount of focus of the density region. We image the movement of the dots in the background, but the interaction that causes the dot movement occurs in the density region. The less of the interaction in the density region we capture through

smaller depth of field, focused only on the background, could correlate to a decrease in image sensitivity in my opinion.

Discussion on BOS sensitivity is continued in Hargather [3]. When we operate within the confines of a predetermined geometrical setup, such as a wind tunnel, we are given a set geometry and desired field of view that often drive the requirements for a camera, lens and background spacing. The lens with the best depth of field that would give the desired field of view would be selected. A camera with large focal length and enough mega-pixels to accurately map the background while still offering a fast enough exposure time for the speed of the flow would be required. Steady flow with constant conditions or unsteady flow, such as in this test, would both require fast exposure times. The size of the background pattern dots and their spacing are made to a scale that provides a dot in the range of 2 to 4 pixels for the camera depth of field and image sensor in use.

The software used in BOS analysis measures the shift of the background between two images. This shift can be between the image without a disturbance and one with a disturbance or between two images with changes in the disturbance. The camera is focused at or near the background pattern. The size and spacing of a pattern on the background is important to allow the software to recognize the edge of a contrasting pattern, then to discern the amount of pixel shift of that pattern in the second image caused by the light diffraction flowing through the density gradient. The analysis of this work only makes a qualitative interpretation of the software image results, but there is an ability to use the software data to make quantitative analysis. The pixel

shifts of the patterns identified by the software are calculated vectors. The data from these vectors can be analyzed for quantitative analysis.

1.3 Existing Work

No BOS work to date has been found that qualifies or quantifies the types of background patterns for optimization in a particular setup. Reviews of previous BOS work use trial and error to find appropriate dot size for the test setup along with using PIV recommendations for approximate pixel size of a particle [6, p. 167]. This recommendation of a 2.5 pixel size dot also applies to spacing between dots for BOS. Raffel's PIV particle size uncertainty has been applied widely to BOS background setup but there has been no effort to validate the pixel size recommendation through testing.

Goldhahn briefly discusses the scaling of the dot pattern for use in his experiment [2]. He mentions that the density of dots was selected so that it would give a dot size of approximately 2.5 pixels for the experimental setup. Other existing work that has been reviewed focuses primarily on applications of BOS, and the selection and use of background patterns have only anecdotal discussions [11].

1.4 Current BOS Research

Most of the current work on BOS deals with applying the techniques to specific test facilities or test series to improve visualization of density gradients. Work at the Arnold Engineering Development Center (AEDC) has dealt predominately with

applying BOS to the available wind tunnels. Reinholtz has adapted BOS to the 16 foot transonic wind tunnel as detailed in [7]. AEDC has an aging infrastructure of wind tunnels and the use of BOS for test data collection has made considerable improvements in the quality and quantity of data obtained. With the success of BOS in the 16 foot wind tunnel, it is now being adapted for use in other wind tunnels and ballistic ranges at AEDC.

BOS has been adapted for large scale outdoor use in testing for explosives research as documented by Biss [1]. In this application it is called Natural-Background-Oriented Schlieren (NBOS). The available natural background is used in this method, and the software analyzes the distortion in the background to predict and image shock wave position.

1.5 Problem Statement

Use of BOS techniques to visualize flow of varying density gradients is slowly becoming used more frequently throughout the research and development world as technology in computing and photography have improved. Researchers continue to use previously used background patterns that have yielded sufficient results without making concerted efforts to find an optimized background pattern for use in BOS. The backgrounds used by previous researchers were developed through simple trial and error methods of using patterns with sufficient contrast to image the density gradients.

While we have seen that many types of background patterns produce acceptable results to visualize the flow, it is not known how well we can improve the visualization of the density gradients by selecting backgrounds that have the proper mix of characteristics as discussed in this thesis.

1.6 Research Objectives

The objective of this research was to develop an initial comparative characterization of variables in a BOS background pattern to guide future research in BOS improvements. The BOS technique has many variables that could be studied for improvement, such as camera, lighting or processing software. For the research in this thesis all variables other than the background were held constant, as much as possible, and the variables within the background pattern were introduced and examined.

The results of this test series were studied primarily in a qualitative manner. The use of the PIV software does offer the possibility of extracting quantitative data for review, but the work of extracting and analyzing that data is beyond the scope of this thesis.

The images obtained from each test series had variables that were changed and compared. The results of those qualitative image comparisons are tabled for review. With the review of the changed variables and the image results, general statements can be made on the variables ability to improve or degrade the quality of the image.

The results of this work is meant to establish a starting point for future research to quantify an improved or optimized background pattern. As discussed previously,

future work could extract data to further quantify results or new test techniques, background patterns and materials could be examined.

II. Methodology

2.1 Overview

In this section we will discuss how the test series was setup and executed. The objective of this test was to hold most variables constant, to the greatest extent possible, while changing predetermined variables of the background pattern to determine their impact on image quality. Between each test series care was given to keep setup parameters alike. This included the parameters of the software used to analyze the image and the parameters of the hardware used to capture the images. These tests were conducted at AEDC with the use of government equipment that was purchased by the flight technology program. This equipment is primarily used in research at AEDC to aid in modernization of the base wind tunnels.

2.2 Test Setup

The tests were conducted at AEDC in the base laser laboratory building. The setup is shown in Fig. 2.1, Fig. 2.2, Fig. 2.3 and Fig. 2.4 below.

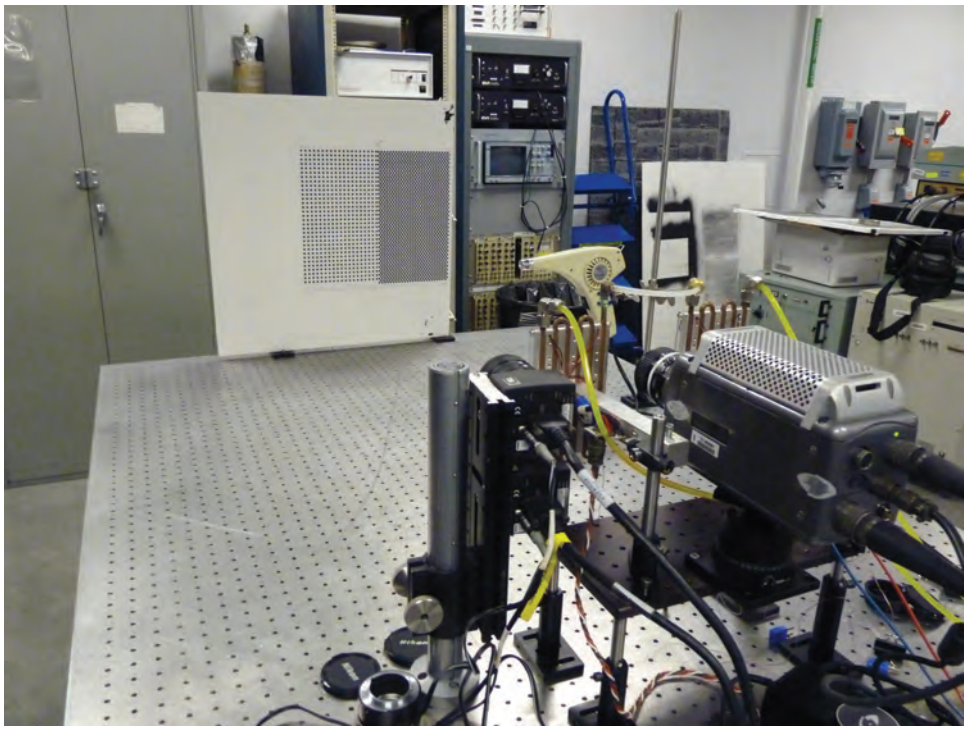

Figure 2.1: View 1 of test setup

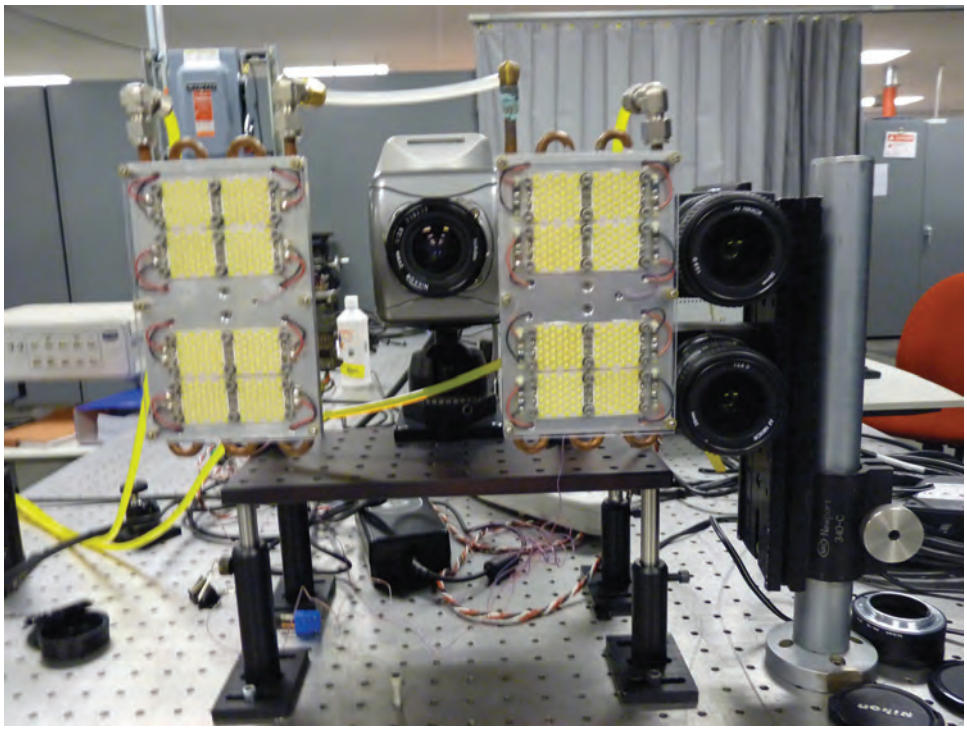

Figure 2.2: View 2 of test setup

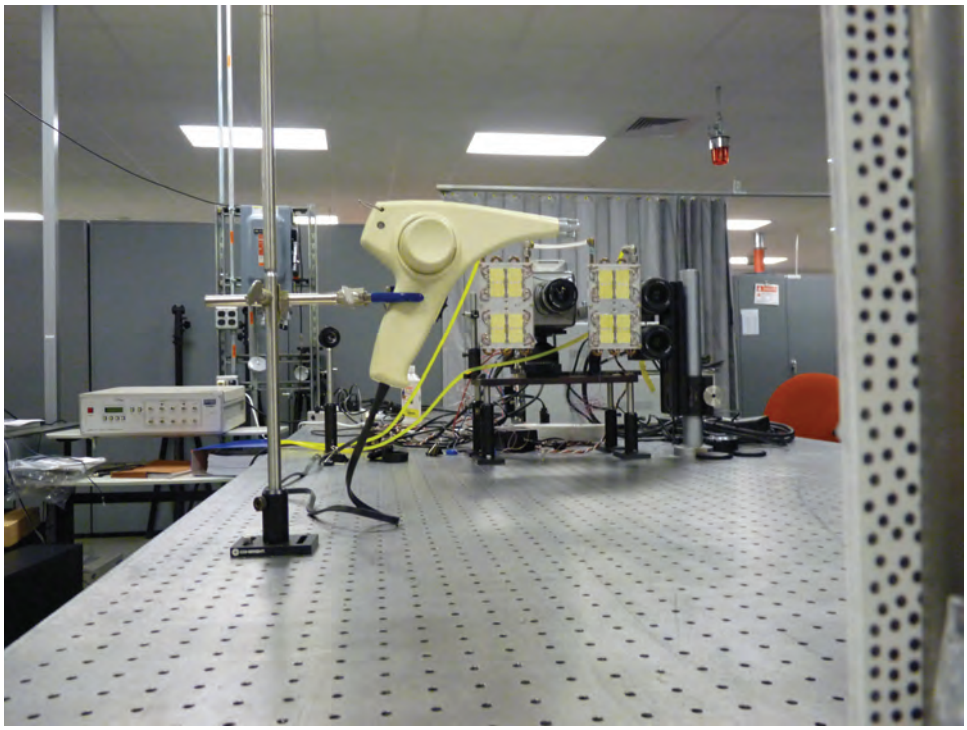

Figure 2.3: View 3 of test setup

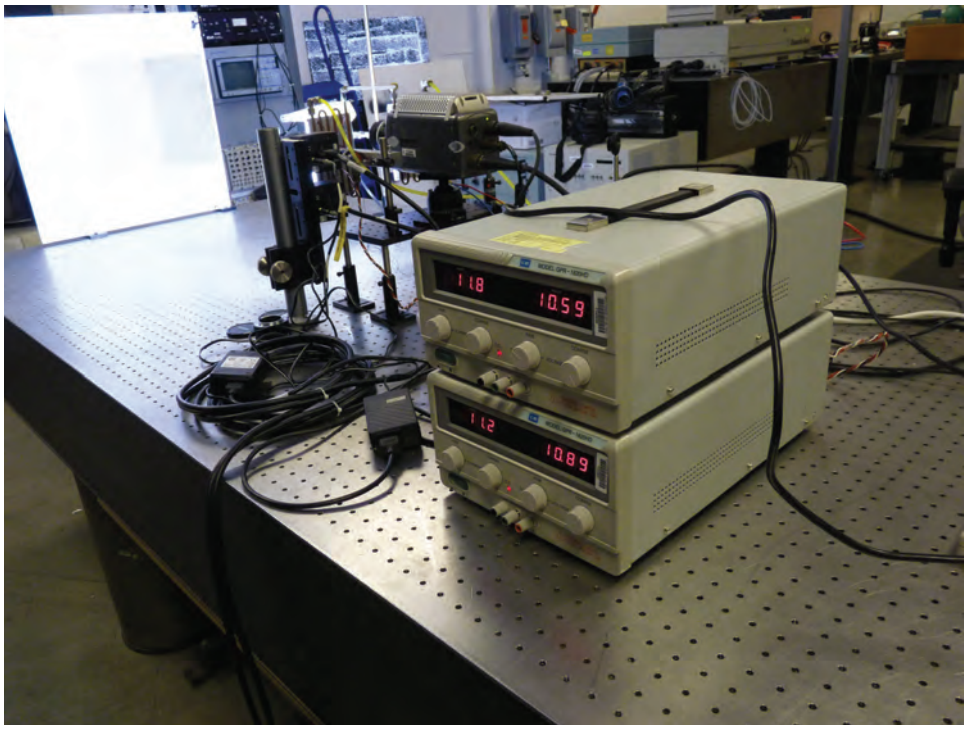

Figure 2.4: View 4 of test setup

The test equipment was installed on a standard Newport optical grade table with vibration isolation. The test equipment was kept in place, without tear down, for the duration of the test. Every effort was made to keep all equipment in its starting configuration to reduce test variability.

The imaging camera used was a Phantom v9.1. The Phantom is a high speed, high resolution camera. For this test, a simple high resolution digital camera was all that was needed. The only camera available for the duration of the test series was the Phantom, so it was used as the primary imaging camera. An expensive high speed Phantom camera is not needed for most BOS imaging. The use of low cost equipment was one of the primary reasons for using BOS vice standard schlieren photography. BOS does have the capability of rendering flow image video with the

use of a camera such as the Phantom. Successive image frames can be taken with a high speed camera, then processed and displayed as video. The ability of BOS to image this kind of high speed, high resolution flow video in near real time is another key attribute.

The camera settings were initially set at standard mid-range settings and held constant throughout the duration of the test series. A standard 28mm focusing lens was installed on the camera. Please note that the additional camera lenses shown in Fig. 2.2 to the right of the camera were not needed or used for this test series. These lenses were used for separate experimentation that was conducted after the test. The exposure rate was adjusted through trial and error at the beginning of the test series. Several exposure times were attempted and an optimal time of 1000 μs was found that worked well with the available lighting in the laser laboratory building. F-stop was set to 4. Camera resolution of 1600 x 1200 was used for all imaging. This was the maximum resolution of the camera.

Lighting for the test was a locally made array of Light Emitting Diode (LED) lighting mounted next to the camera, as seen in Fig. 2.2. LED lights were available for the test and were used to provide a consistent lighting source between the two cross correlated images captured during testing. The low speed flow did not require very small exposure times. Therefore, the LED light provided ample lighting for the chosen exposure time. The LED lights were locally made here at AEDC for confined lighting needs. Each LED panel had an array of 8 Lamina® BL-3000™ white light, approximately 5500K, LED strips that were powered with adjustable

Figure 2.5: LED lighting cooling water chiller

voltage regulators as shown in Fig. 2.4. Voltage to the LED panels was held at 11 volts per panel during the duration of testing. Each LED panel was liquid cooled to prevent overheating and light output degradation during long lighting periods. Liquid cooling was provided by a RTE-110 chiller shown in Fig. 2.5.

The background was set at a distance of 4 feet from the camera. This distance simulated a mid-size wind tunnel configuration such as the AEDC 4T wind tunnel. The background was a 4 foot square foam backed poster board, which was used to attach the various trial patterns.

The density gradient was created by a standard shop heat gun mounted midway between the camera and the background at 2 feet as shown in Fig. 2.3. This would simulate a test article in the middle of the tunnel. The heat gun had a blower that blew the hot air across the field of view. The trial background test patterns were placed, one on top the other, on the foam board. Two test patterns were compared

side by side at each test to allow for comparison. The heat gun was aligned to blow over the middle of each test pattern so that any difference in image quality could be easily discerned. Flow from the heat gun was unsteady and turbulent. This remained relatively consistent between tests for pattern comparison, but still provides some lack of continuity. The heat gun was chosen because it was readily available and it was easily set up. Ideally a more consistent diffraction technique, such as simple glass diffraction, could have provided more consistent test conditions between tests. The alignment of camera, lighting, heat gun and background can be seen in Fig. 2.6. This is an overhead view that shows the 4 foot camera to background setup with the target density gradient midway.

For data analysis, images were transferred directly from the Phantom camera to a local computer with PIV processing software installed. The software used for analysis on this project was LaVision® DaVis™ v7.2. The cost for a license of PIV software like this is substantial and could easily be one of the higher project costs when initially setting up a BOS system. AEDC held current licensing for this software and the multi-core processor computer on which it was installed was readily available. The DaVis™ software was used to calculate the displacement vectors of the dots change in position between cross correlated frames. The software can image results in many styles, but for the processing in this thesis, primarily schlieren style imaging showing bright and dark intensity levels was used. The brighter shades on the processed image indicate larger magnitude dot displacements between evaluated image pairs and the

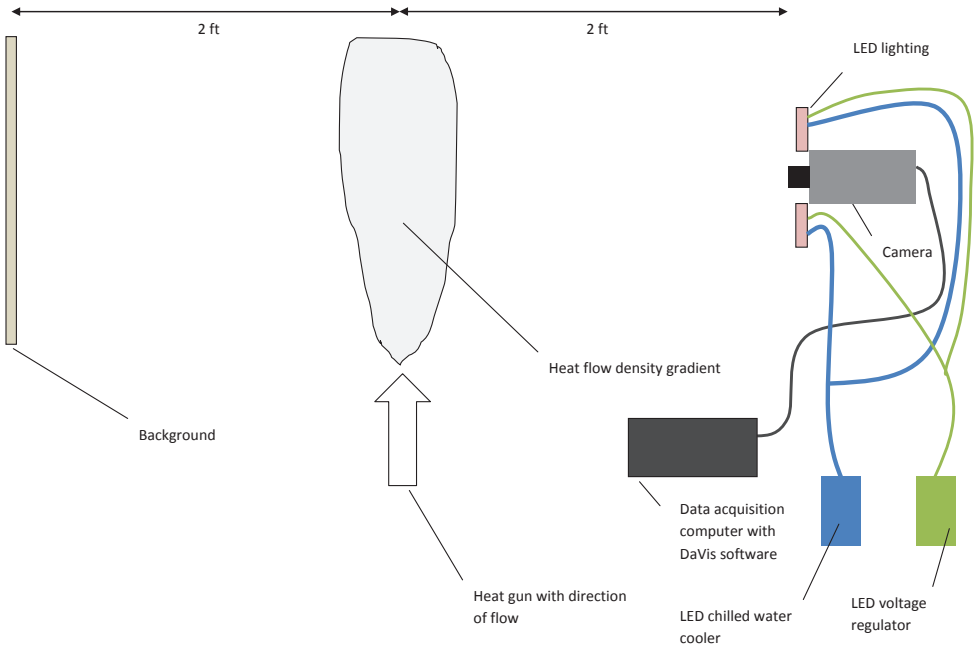

Figure 2.6: Overhead drawing of test setup

darker shades indicate smaller displacements. These dot displacements between image pairs correspond to changes in the density gradient of the flow.

To process the images with the DaVis^{TM} software, raw images were directly imported from the imaging camera as single images. Then the images were paired together for each test to process. Standard PIV processing was applied. The interrogation region chosen was 16 x 16 pixels along with a 50% region overlap. This interrogation region was selected through trial processing using test pattern 1. A larger interrogation region would have offered smaller uncertainty, as seen in Fig. 1.5, but would have added considerably more processing time for the software solution. The amount of uncertainty added by using the smaller interrogation region was considered acceptable as long as it was held constant throughout the processing of all test series. The overlap corresponds to a re-do of a specified percentage of the interrogation region. For instance, when the software scans a 16 x 16 pixel region it does not start immediately on the next region. Instead, it goes back into 50% of the previously completed region and starts from there. The size of the interrogation region and overlap affect sensitivity of the image. For larger standoff distances and larger background dot sizes, larger interrogation regions would be prudent to capture the dot movement between cross correlation of images. For these tests the processing parameters were held constant to minimize their impact on the results.

The background patterns used were simple black and white images of repeated shapes. The shapes tested were circles, triangles, squares and hexagons. Any number of different style shapes could have been used, but this small selection of shapes

was thought to give enough variety to determine if shape variation influenced image quality. In previous BOS work the typical shape used was a circular dot. It is thought that the shape of the pattern will matter little to the sensitivity of the image, but no BOS work has ever tested this theory. These tests will attempt to validate the assumption made in previous work that circular dot shapes provide the best image quality possible. The size of the shape was varied on some patterns and the spacing between the shapes was also varied.

A total of 21 separate background test patterns was made. 11 patterns with circular dots, 4 patterns with triangles, 4 patterns with hexagons and 2 patterns with squares. The patterns used for testing can be seen in Table 2.1. Size of the shapes varied between 0.05" and 0.5". Spacing between the shapes varied between 0.05" and 0.6" on horizontal and vertical axis. Additional spacing variation was given by leaving rows aligned in a grid like pattern or offsetting alternating rows to reduce spacing.

A typical view of the background patterns that was developed for testing is shown in Fig. 2.7 and Fig. 2.8. These pictures show the difference in spacing between the grid and offset patterns. Test series were developed to test these patterns side by side for close comparison. Test series placed background patterns with different shapes side by side for comparison, patterns with different sized shapes side by side for comparison and patterns with different spacing between shapes side by side for comparison. The analysis of this matrix of test patterns should produce results that

Table 2.1: Background patterns

Pattern Number	Shape	Size	Spacing (offset or grid)
1	Circle	0.2"	0.1" horizontal 0.0" vertical offset
2	Circle	0.1"	0.1" horizontal 0.0" vertical offset
3	Circle	0.1"	0.1" horizontal 0.1" vertical grid
4	Circle	0.2"	0.2" horizontal 0.2" vertical grid
5	Circle	0.05"	0.05" horizontal 0.05" vertical grid
6	Circle	0.05"	0.05" horizontal 0.0" vertical offset
7	Circle	0.3"	0.3" horizontal 0.0" vertical offset
8	Circle	0.3"	0.3" horizontal 0.3" vertical grid
9	Circle	0.5"	0.5" horizontal 0.0" vertical offset
10	Circle	0.5"	0.5" horizontal 0.5" vertical grid
11	Circle	0.2"	0.6" horizontal 0.2" vertical offset
12	Triangle	0.2"	0.1" horizontal 0.0" vertical offset
13	Triangle	0.1"	0.1" horizontal 0.0" vertical offset
14	Triangle	0.1"	0.1" horizontal 0.1" vertical grid
15	Triangle	0.2"	0.2" horizontal 0.2" vertical grid
16	Hexagon	0.2"	0.1" horizontal 0.0" vertical offset
17	Hexagon	0.1"	0.1" horizontal 0.0" vertical offset
18	Hexagon	0.1"	0.1" horizontal 0.1" vertical grid
19	Hexagon	0.2"	0.2" horizontal 0.2" vertical grid
20	Square	0.1"	0.1" horizontal 0.1" vertical grid
21	Square	0.2"	0.2" horizontal 0.2" vertical grid

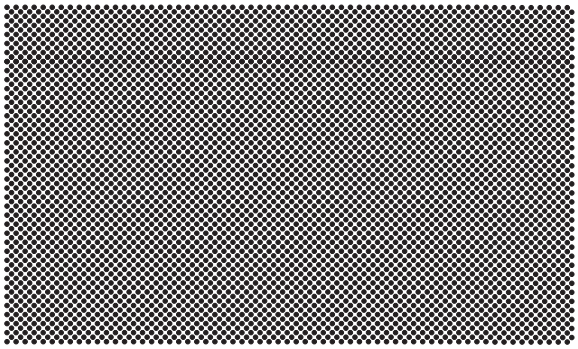

Figure 2.7: View of typical offset background pattern used during testing

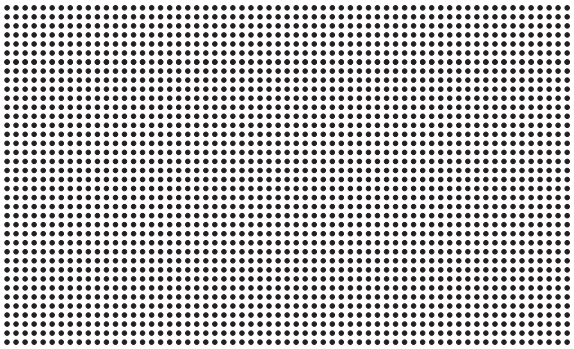

Figure 2.8: View of typical grid background pattern used during testing

can definitively show if the variation in the isolated parameter improves or degrades image quality.

Before testing an estimate for the expected optimal pattern size was calculated using the PIV recommendation shown previously in Fig. 1.5 and the geometry in the test setup. The density gradient area of interest was approximately 14" x 10" rectangular which translated to a background area of approximately 28" x 20" rectangular. The camera was set at 1600 x 1200 pixel resolution. When we take the width of the rectangle along with the 1600 pixel width the result is shown in Eq. 2.1.

$$28" \div 1600\, pixels = 0.0175\, \frac{inch}{pixel} \times 3\, pixel\, recommendation \approx 0.053" \qquad (2.1)$$

Therefore, for the setup geometry in tests 4 through 24, we would expect a dot size of approximately 0.05" to be near optimal.

2.3 Test Execution

For the execution of the test series a test matrix was used. This matrix is shown in Table 2.2. The matrix was developed to isolate the shape, size and spacing variables respectively with a few of the later test series comparing size and spacing variables combined.

Tests 1, 2 and 3 had baseline backgrounds without numbering, but are further described in the next section. Tests 4, 5 and 6 are variations in setup using the same patterns and are discussed more in chapter 3. Test 26 used a unique stamped pattern that was not numbered, but is discussed more in chapter 3.

2.4 Test Baseline Series

The first 3 tests were baseline images to verify poor image quality in the absence of structure on the background and how adding small amounts of structure begins to allow the software the ability to map reference points between images. These

Table 2.2: Test matrix for background patterns

Test Number	Pattern Numbers	Parameter Evaluated
1	Baseline with white background	None
2	Baseline with black background	None
3	Baseline with black and white grid pattern	None
4	1 and 4	Spacing
5	1 and 4	Spacing
6	1 and 4	Spacing
7	1 and 11	Spacing
8	1 and 12	Shape
9	1 and 16	Shape
10	1 and 2	Size
11	2 and 3	Spacing
12	2 and 13	Shape
13	2 and 17	Shape
14	3 and 14	Shape
15	3 and 20	Shape
16	3 and 18	Shape
17	4 and 15	Shape
18	4 and 21	Shape
19	4 and 19	Shape
20	5 and 6	Spacing
21	5 and 3	Size and Spacing
22	6 and 2	Size and Spacing
23	7 and 8	Spacing
24	9 and 10	Spacing
25	Plate 1 and Plate 2	Size and Spacing
26	Various vertical patterns	Color contrast

tests were used as a basis to justify the necessity of some type of structure on the background.

Test 1 is shown in Fig. 2.9. The upper image is a raw unprocessed image of the background with no density gradient present. The lower image is a processed cross correlation of the upper image and a second image with the density gradient present. The lower processed image shows the PIV software imaging of the change in position of the dots located on the background, or the shift, $\triangle x$ and $\triangle y$, of the dot from frame one to frame two. The magnitude and direction the dots displacement in the second cross correlated image corresponds to changes in the density gradient of the flow from the first photo to the second. The light intensity of the processed flow imaged is proportional to the magnitude of the change in position of the dots in the background. Higher magnitudes of dot displacement result in brighter mapping of the flow in the processed image. This test was an attempt to image on a white background with no structure. As you can see by the image, the software was not able to discern points between the air off image and the air on image to provide any view of the density gradient. This shows the inability of DaVis^{TM} software to map density gradients on a solid white background with no structure. Without the structure of some contrasting point on the background, the software is incapable of creating a reference point for comparison, even when the density gradient is present. During an air on event the light is passing through the gradient and is still being bent at an angle of ε, as shown previously in Eq. 1.4. But now, with a lack of contrasting structure on the background, the software is not able to reference that light shift and map it

to the image. Notice the complete lack of a density gradient in the second processed image. The image does show an area in the center section that differs from the rest of the background. This correlates to how the camera, centered on the middle of the background, sees the light rays head on in a straight line vice angled toward the outer edges.

Test 2 was similar to test 1 with a lack of background structure, but the color was changed to black. Test 2 is shown in Fig. 2.10. Once again we see that a lack of structure provides no means for the software to differentiate between points in the air on and air off images. Flows of the density gradients are not able to be imaged by the software. The lack of change in quality between the changing of background colors is expected. The primary means for the software to pick out a target on the background is contrast. Changing the background or dots to other colors would not provide an increase in sensitivity of the processed BOS images unless it increased the contrast between the two. With the combination of black and white offering the largest change in contrast available, it should always provide the best background. A black background with white dots or a white background with black dots would make no difference. The contrast between the two is the key factor. This was also verified in test 26 shown later in Fig. 3.26

Test 3 is a black background with a 1 inch white grid pattern running both vertical and horizontal. This test shows a slight improvement from tests 1 and 2 where no pattern was present. This image does not have nearly enough structure for the software to image well, but does show that adding some structure allows

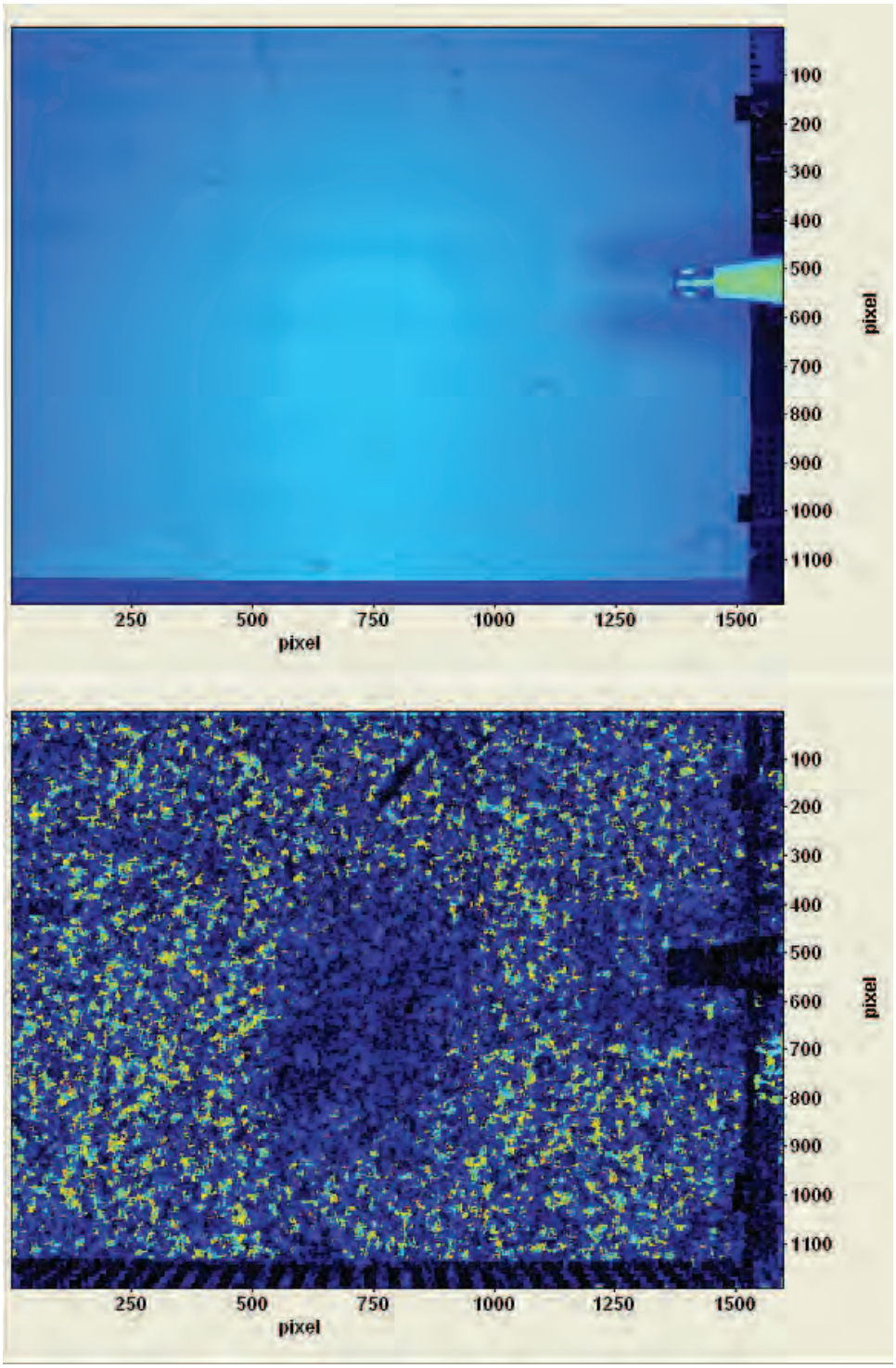

Figure 2.9: Test 1 using a white background with no structure

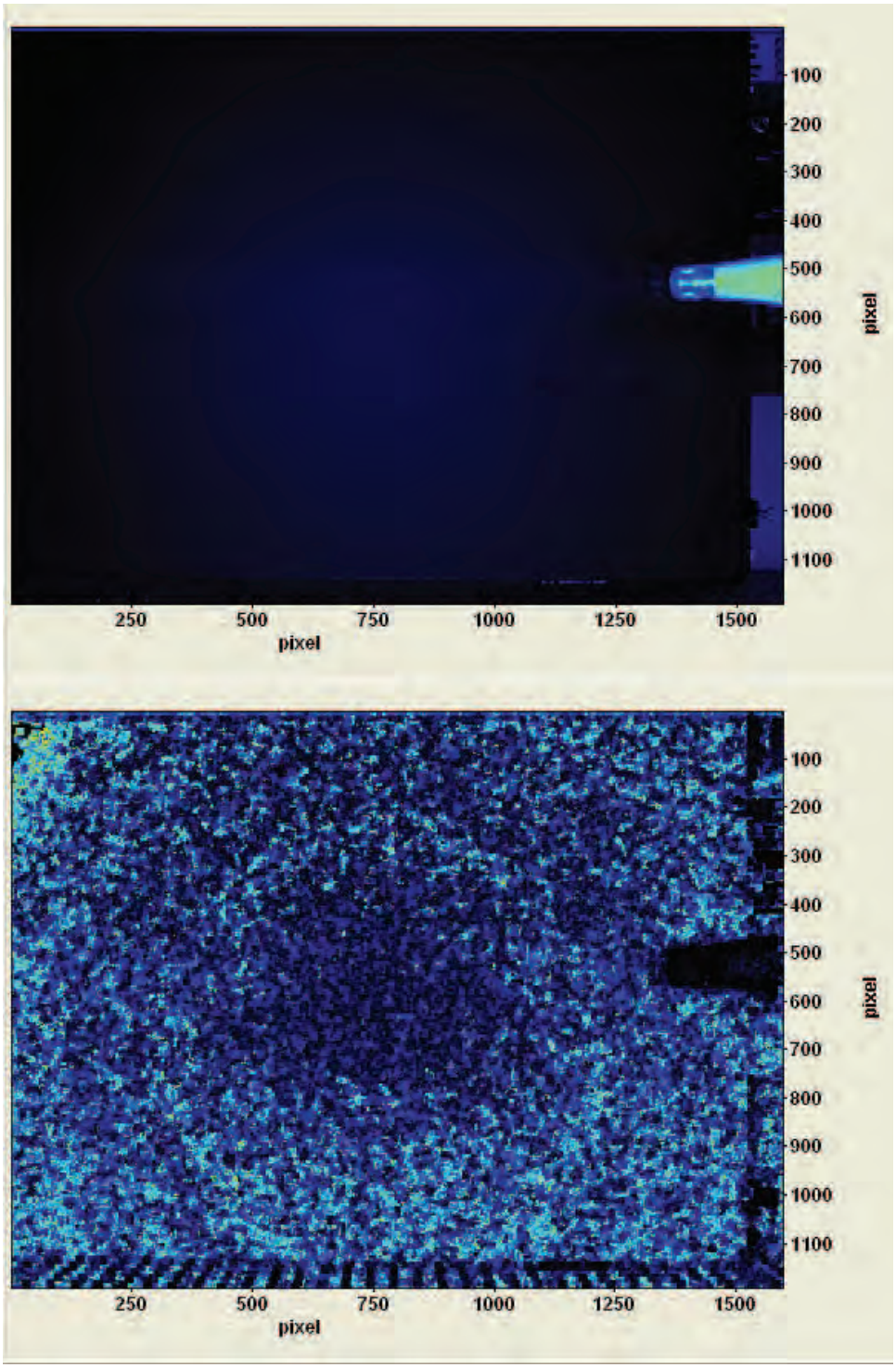

Figure 2.10: Test 2 using a black background with no structure

the software to begin to find reference points for comparison between images. It is difficult to see much improvement between test 3 and tests 1 and 2, but when you zoom closely at test 3, you can see faint traces of density gradient flows. The large square sections within the grid that lack pattern do not return any density change and give the image an overall lack of density change. Test 3 is shown in Fig. 2.11. The small traces of the density gradients are visible at the grid lines when you zoom in on the image.

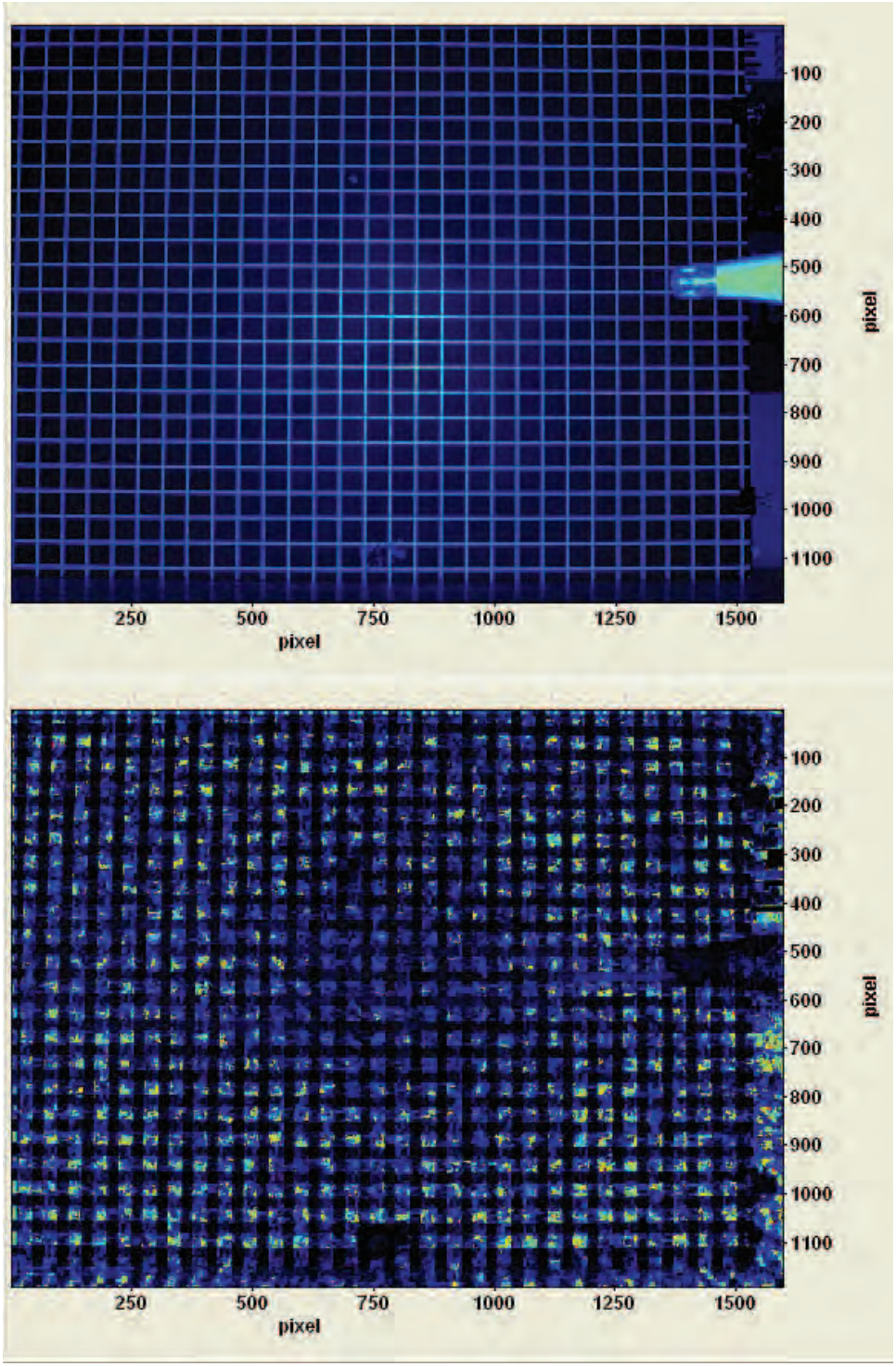

Figure 2.11: Test 3 using a black background with minimal structure of horizontal and vertical lines

III. Results and Analysis

3.1 Summary of Results

The results of the test series are summarized in Table 3.1, Table 3.2 and Table 3.3. The tabled results summarize changes or lack of changes in image quality between the compared patterns. Results of the tests show significant variation in image quality with the size and spacing of the shapes on the background pattern while showing no change in image quality with the type of shape used. These results correlate well with conventional thinking in BOS setup that a major factor in background optimization is high contrasting of closely spaced dot patterns. Most tests showed that smaller shapes grouped closely together, up to a certain point, gave the software more finely meshed reference points for comparison. The point at which size and spacing appeared optimized for this setup is discussed in the next section.

Large scale images of the test series are placed in this chapter for easier viewing. When viewing the test images, comparisons were made between the detail of the flow characteristics between the upper and lower patterns. Some tests showed significant image quality variations between patterns while other tests showed no difference in image quality between patterns. The raw images reviewed were high resolution. This allowed for fine zoom in of the flow to evaluate poorer image quality with more pixel blur.

Table 3.1: Results of Spacing Variable

Test Number	Spacing With Best Image (Large, Small or No Difference)
4	Small
5	Small
6	Small
7	Small
11	No Difference
20	No Difference
21	Small
22	Small
23	Small
24	Small
25	Small

Table 3.2: Results of Size Variable

Test Number	Size With Best Image (Large, Small or No Difference)
10	Small
21	Small
22	Small
25	Small

Table 3.3: Results of Shape Variable

Test Number	Shape With Best Image (Circle, Triangle, Square, Hexagon or No Difference)
8	No Difference
9	No Difference
12	No Difference
13	No Difference
14	No Difference
15	No Difference
16	No Difference
17	No Difference
18	No Difference
19	No Difference

3.2 Analysis of Processed BOS Imaging

This section reviews each of the main test series with large images for easier viewing. Each test image is commented with setup criteria along with results analysis.

Tests 4, 5 and 6 were used to determine best placement and alignment of the heat gun and the background patterns. For these tests, patterns 1 and 4 were used. Orientation of the patterns was changed from vertical in test 4, to horizontal in tests 5 and 6. With the patterns vertical in test 4 the heat gun was positioned so that it blew across the first pattern then across the second pattern. This alignment did not work as well for imaging due to the large change in the density field as the heat leaves the heat gun. Initially when the hot air leaves the heat gun it is relatively focused and has a straight stream. The farther the air flow gets from the heat gun the more it disperses and rotations occur. This would make comparison between the patterns more difficult. It would be very hard to compare the quality of the image over one pattern when the flow was focused and straight, and then dispersing with rotations over the next pattern. The horizontal alignment proved to work much better for a side by side comparison of the patterns. With the horizontal pattern alignment, the heat gun was centered between the patterns so that each side saw and equal amount of flow while the flow dispersed equally over each pattern.

The remainder of the testing, tests 7 through 25, were carried out as mentioned above with horizontal images placed side by side with the heat gun blowing centrally down the axis between the two patterns.

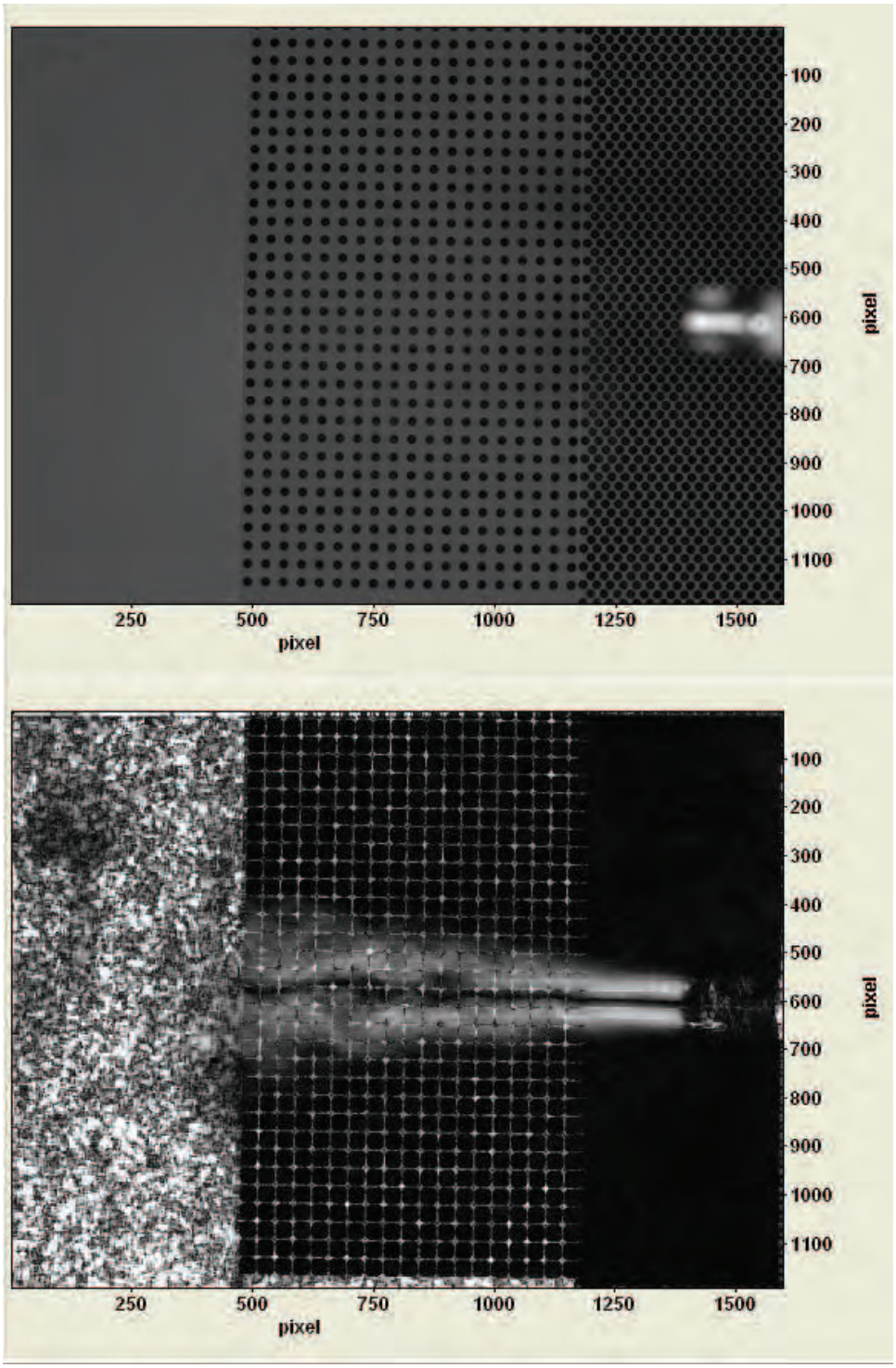

Figure 3.1: Test 4 using patterns 1 to the right and 4 to the left

Fig. 3.1 compares pattern 1, 0.2" dot with 0.1" horizontal and 0.0" vertical offset spacing, against pattern 4, 0.2" dot with 0.2" horizontal and 0.2" vertical spacing. This test evaluated the spacing variable. Orientation of the patterns were vertical instead of horizontal on this test. It was determined after this test that vertical orientation was not conducive to similar flow over each pattern. Therefore, tests 5 through 25 have the patterns in a horizontal orientation to allow for symmetrical flow over both patterns concurrently. Results show better resolution over pattern 1, on the right, with the smaller spacing. The results of this test was omitted from the results table due to test 6 comparing the same patterns. Notice the heat gun is not in focus while the background is in focus. The lens did not have the depth of focus to keep both the background and density region in focus. As mentioned previously, I would have preferred to have a lens capable of focusing on both, but it was not available. This argument for large depth of field is not well understood in BOS applications and has not been tested.

Fig. 3.2 compares pattern 1, 0.2" dot with 0.1" horizontal and 0.0" vertical offset spacing, against pattern 4, 0.2" dot with 0.2" horizontal and 0.2" vertical spacing. This test evaluated the spacing variable. This uses the same patterns as test 4 but places them in a horizontal orientation instead of vertical. Results here again show better resolution over pattern 1 on the bottom of the processed image with the smaller spacing. The horizontal arrangement of the patterns show a near symmetrical flow over each pattern that provides better qualitative results to support the claim

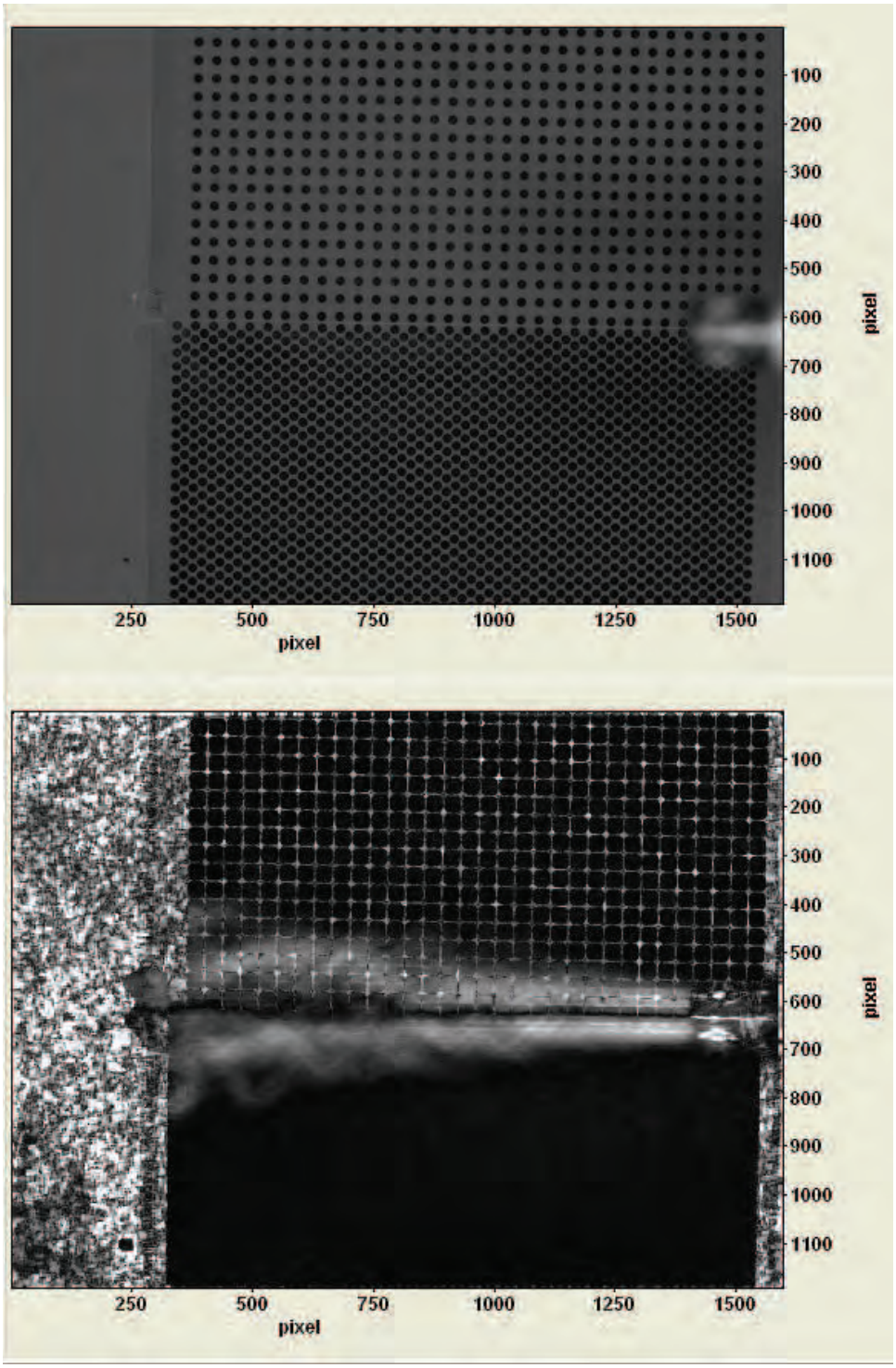

Figure 3.2: Test 5 using patterns 1 on bottom and 4 on top

of better image quality of one pattern over the other. The results of this test was omitted from the results table due to test 6 comparing the same patterns.

Fig. 3.3 compares pattern 1, 0.2" dot with 0.1" horizontal and 0.0" vertical offset spacing, against pattern 4, 0.2" dot with 0.2" horizontal and 0.2" vertical spacing. This test evaluated the spacing variable. This pattern again uses patterns 1 and 4, but here the heat gun was changes to a larger model. The heat gun used in tests 1 through 5 was not available so another heat gun was used. This heat gun had a larger exit nozzle that worked quite well for testing. The larger diameter nozzle allowed for the flow to cover more of the upper and lower patterns. This allowed for more BOS imaging over each pattern to give more area for qualitative analysis. Similar to test 4 and 5, results of these patterns show better resolution of the flow over pattern 1 on the bottom with the smaller spacing.

Fig. 3.4 compares pattern 1, 0.2" dot with 0.1" horizontal and 0.0" vertical offset spacing, against pattern 11, 0.2" dot with 0.6" horizontal and 0.2" vertical offset spacing. This test evaluated the spacing variable. Pattern 1 on the bottom with the smaller spacing showed significantly better image quality. Pattern 11 on the top with large spacing had areas between the dots where imaging of the density gradient was lacking.

Fig. 3.5 compares pattern 1, 0.2" dot with 0.1" horizontal and 0.0" vertical offset spacing, against pattern 12, 0.2" triangle with 0.1" horizontal and 0.0" vertical offset spacing. This test evaluated the shape variable. No appreciable difference can

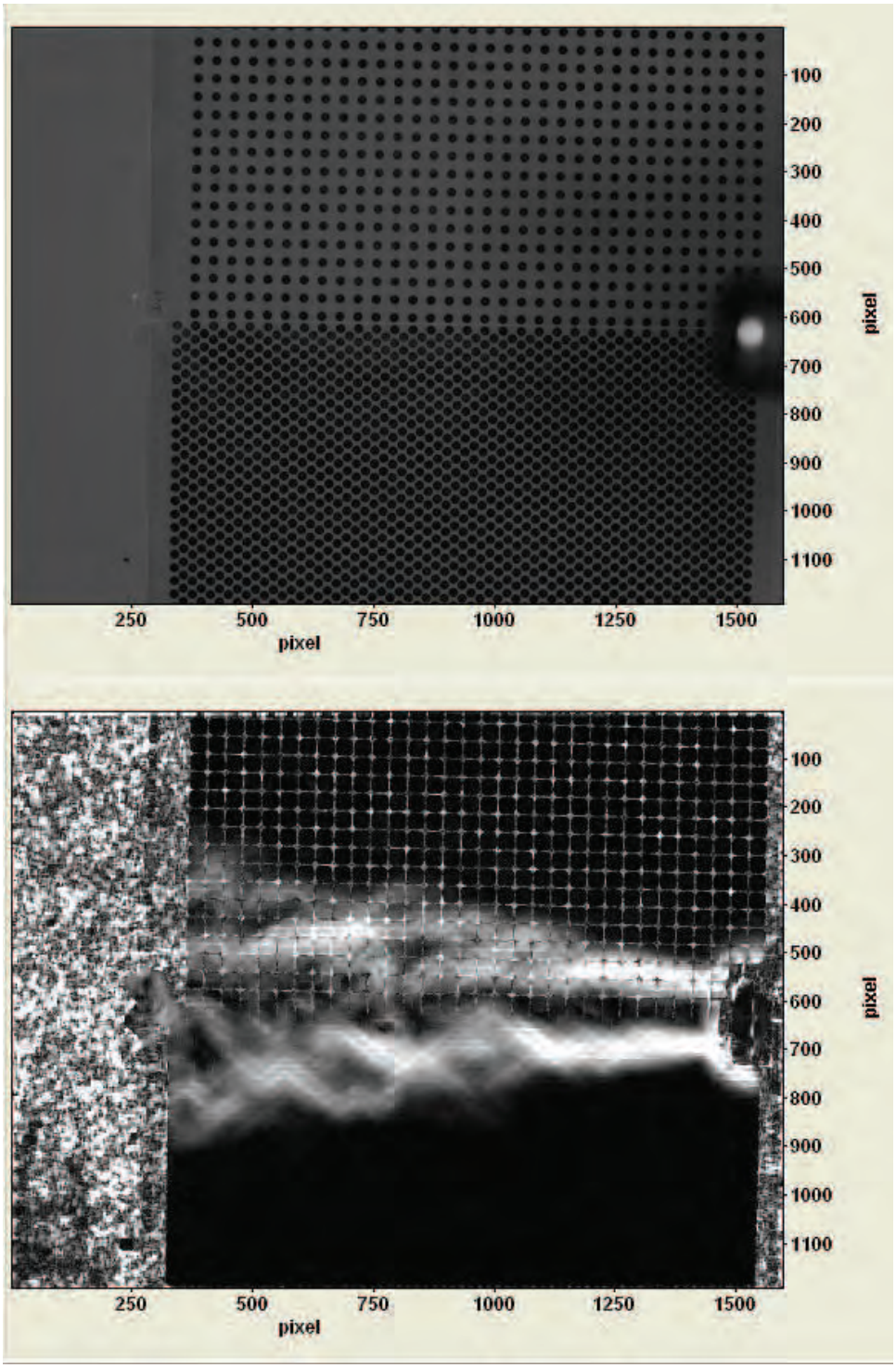

Figure 3.3: Test 6 using patterns 1 on bottom and 4 on top

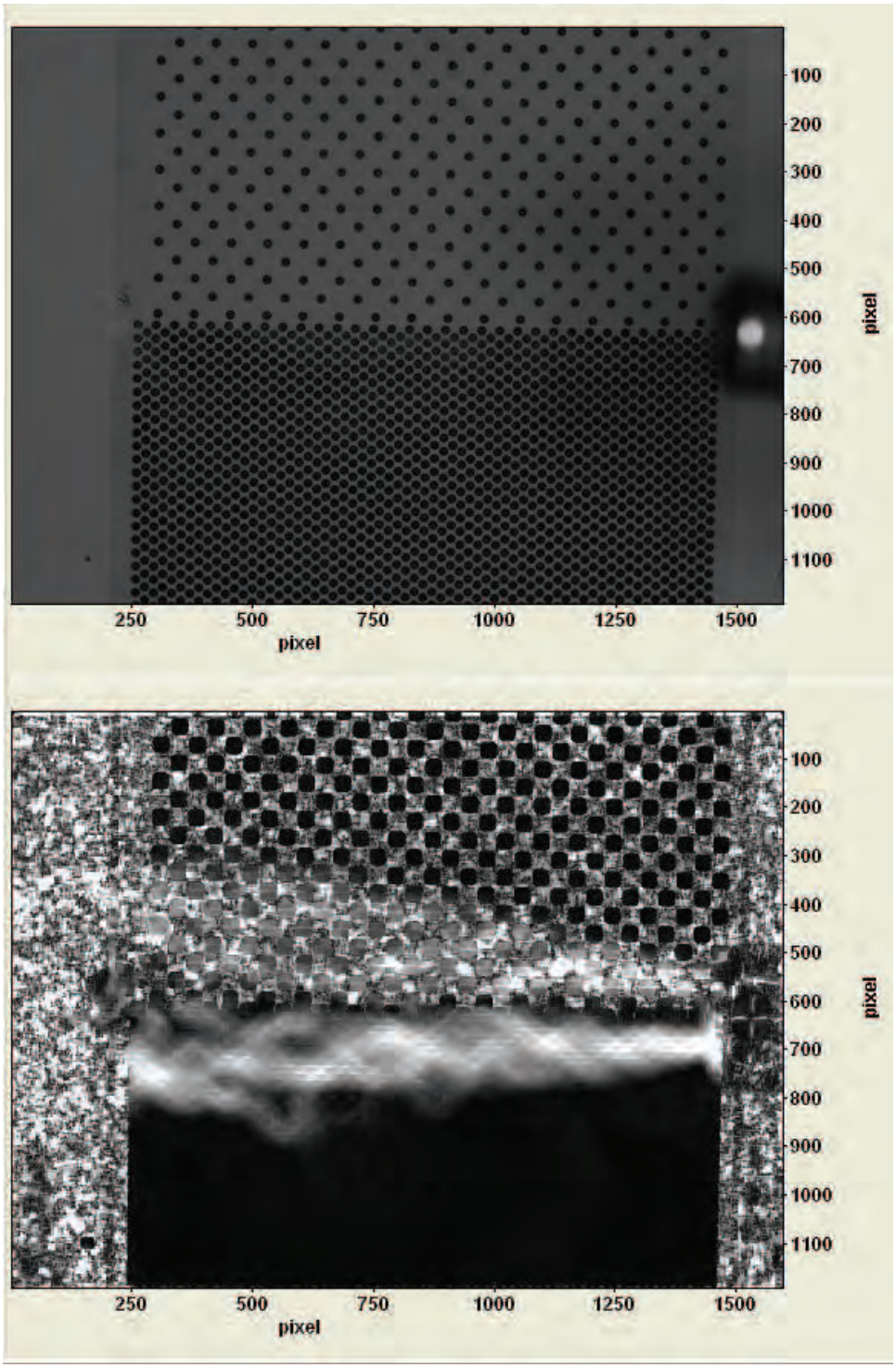

Figure 3.4: Test 7 using patterns 1 on bottom and 11 on top

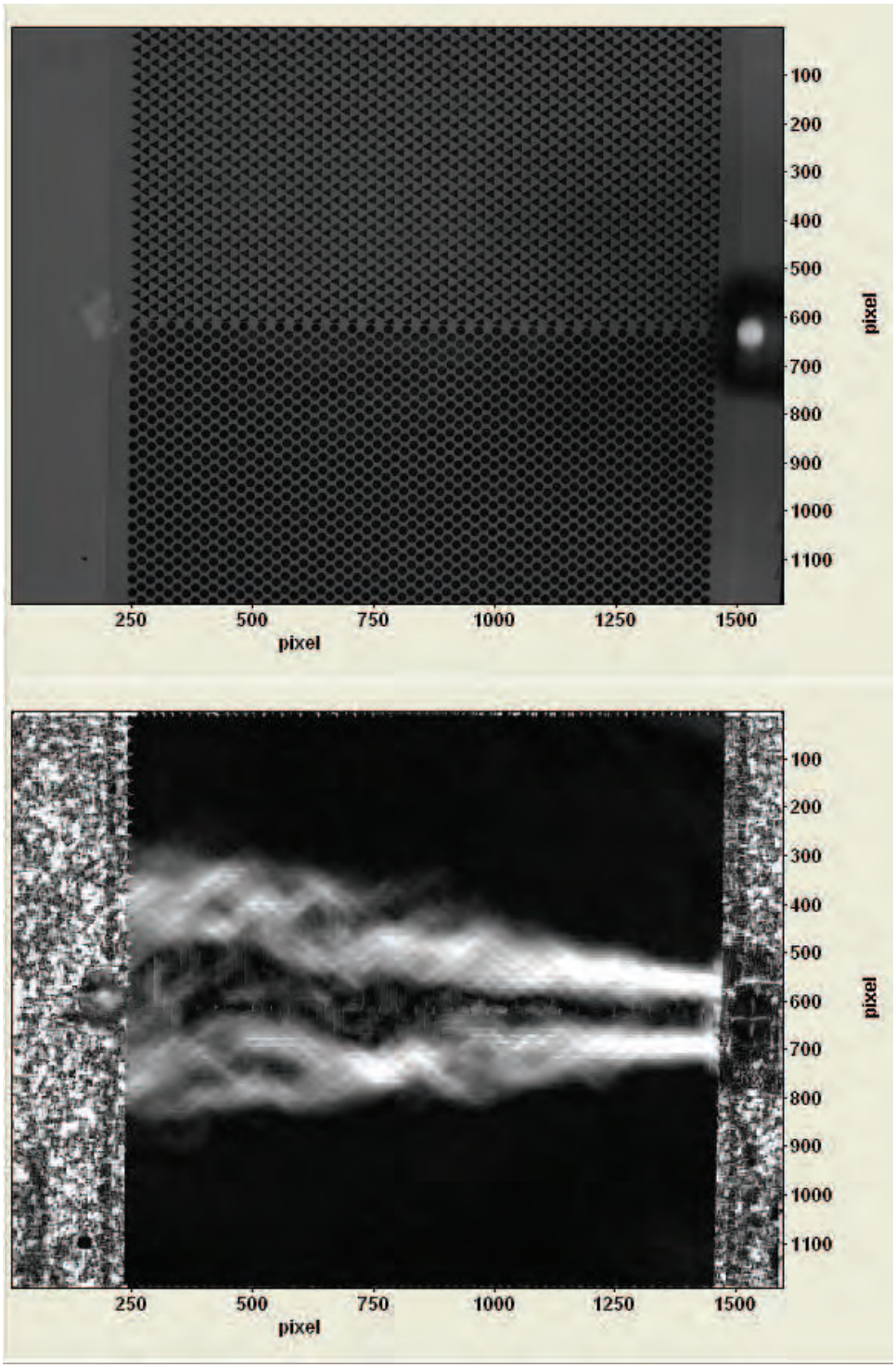

Figure 3.5: Test 8 using patterns 1 on bottom and 12 on top

be seen between both patterns. Similar spacing and pattern size appear to produce similar image quality results of the density gradients in both the upper and lower images.

Fig. 3.6 compares pattern 1, 0.2" dot with 0.1" horizontal and 0.0" vertical offset spacing, against pattern 16, 0.2" hexagon with 0.1" horizontal and 0.0" vertical offset spacing. This test evaluated the shape variable. No appreciable difference can be seen between the patterns. Similar spacing and pattern size appear to produce similar image quality results of the density gradients between the upper and lower patterns. Of note on this test is the appearance of lines on the upper right portion of the upper pattern that resemble flow. The appearance of this anomaly can be seen in some of the other tests following this one. It is primarily seen in the upper pattern. The reason for the anomalous patterns in this region are unknown. It is possible they are related to lighting or camera alignment.

Fig. 3.7 compares pattern 1, 0.2" dot with 0.1" horizontal and 0.0" vertical offset spacing, against pattern 2, 0.1" dot with 0.1" horizontal and 0.0" vertical offset spacing. This test evaluated the size variable. This test revealed better imaging over pattern 2 on the top with the smaller size dot. Flow over this pattern has significantly more detail of the density gradient.

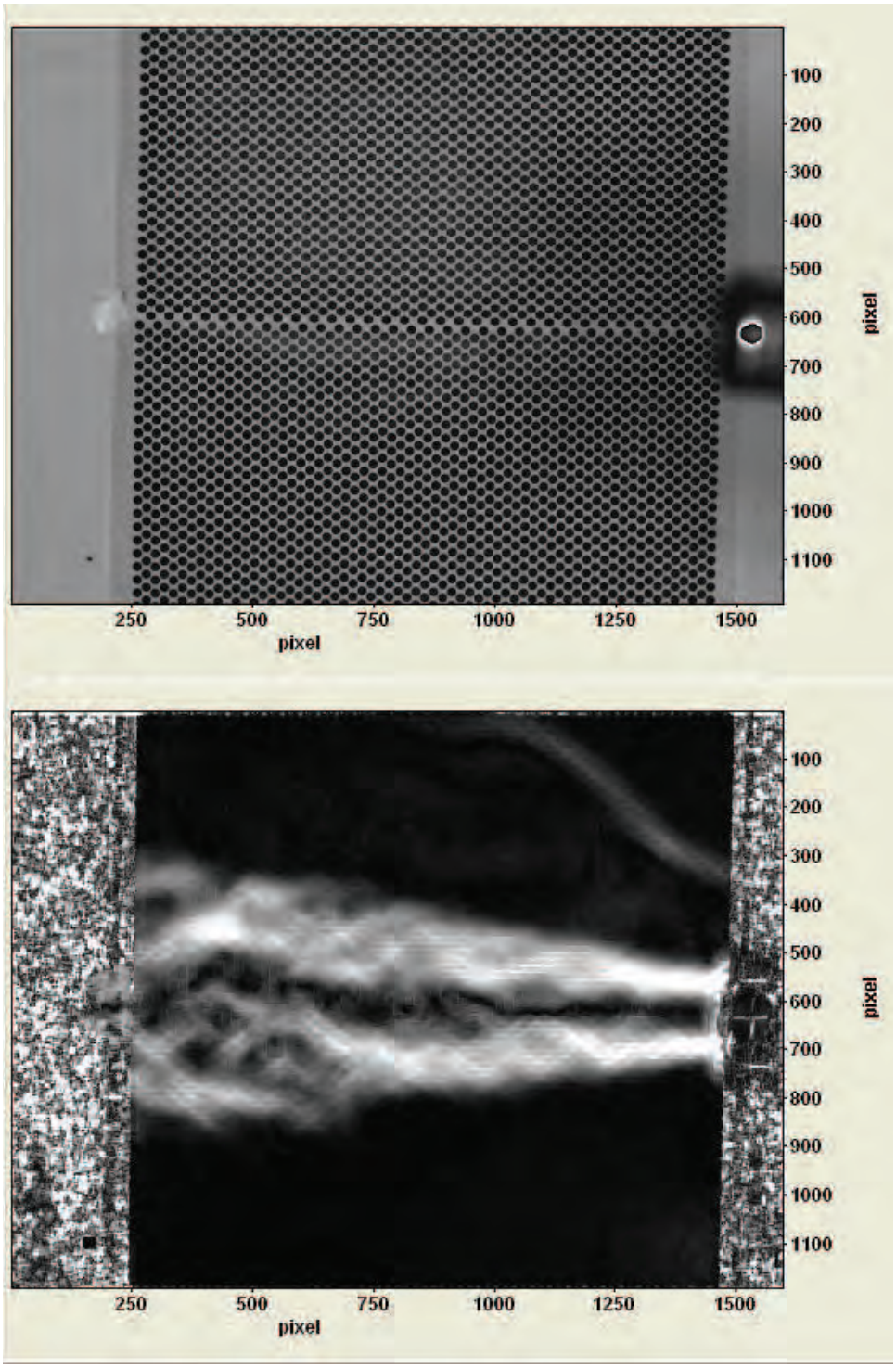

Figure 3.6: Test 9 using patterns 1 on bottom and 16 on top

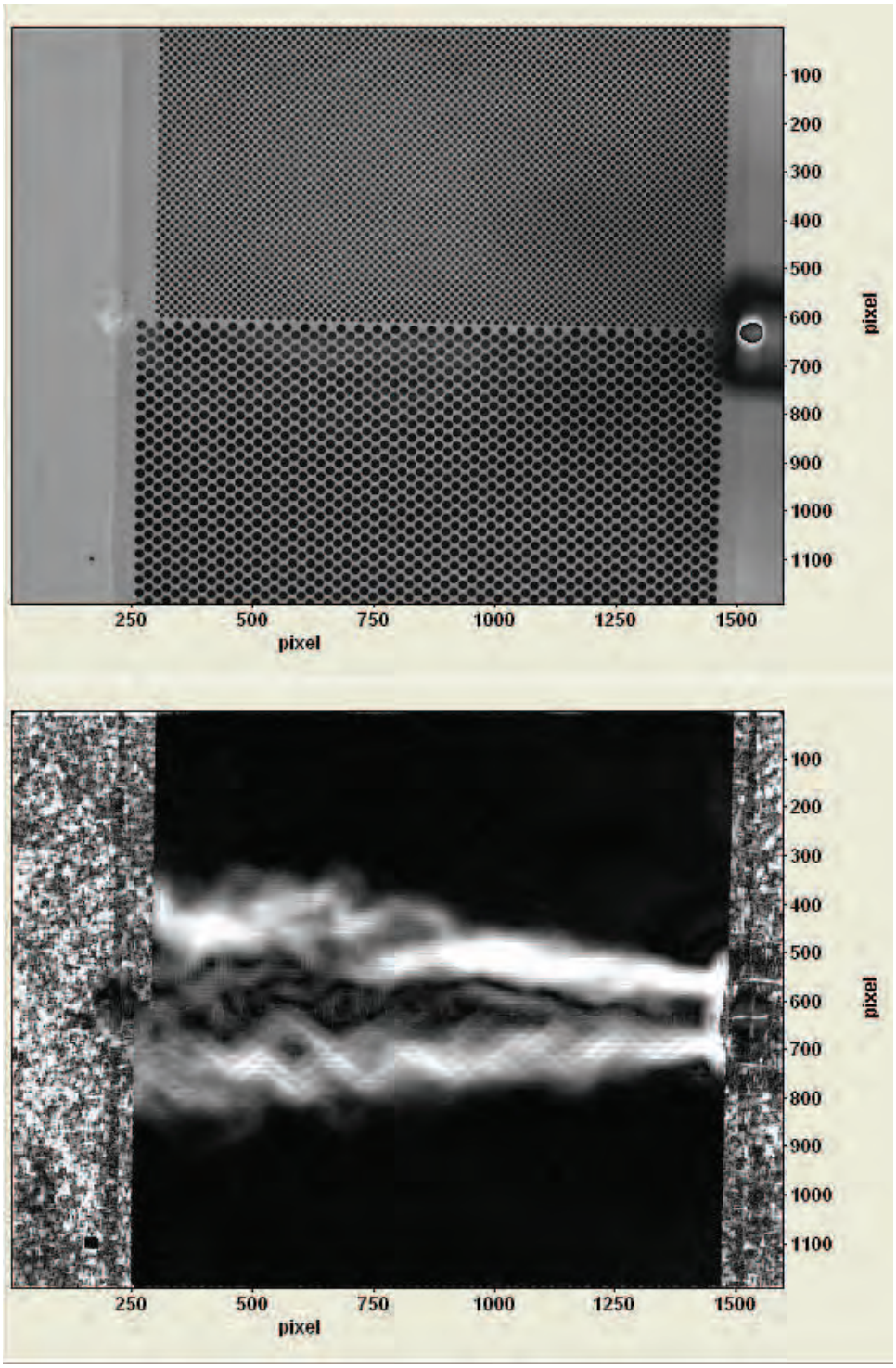

Figure 3.7: Test 10 using patterns 1 on bottom and 2 on top

Fig. 3.8 compares pattern 2, 0.1" dot with 0.1" horizontal and 0.0" vertical offset spacing, against pattern 3, 0.1" dot with 0.1" horizontal and 0.1" vertical spacing. This test evaluated the spacing variable. This test revealed no discernable difference between patterns. Size and spacing of the dots are similar enough to produce like imaging at this distance and image size. Additionally, imaging of the flow can be seen on the far left, past the dot pattern, over the scotch tape used to hold the patterns to the board. This can be seen in many of the other tests, but shows up well here. This is an indication of how different materials used in the background can produce reflectivity that is conducive to better imaging. This is discussed in the next chapter in the recommendations for future work section. New backgrounds made of scotchlite, or other similar type materials, can offer varying light reflectivity that provide quality imaging without additional dot patterns over them. The additional reflectivity of the material can also reduce the required lighting necessary or reduce the need for lowering the f-stop to allow more light in to the sensor. The use of this type of material of course depends on the distance from the background and the size of the test region. A test in a large scale wind tunnel with large stand off would still need a fairly large dot pattern.

Fig. 3.9 compares pattern 2, 0.1" dot with 0.1" horizontal and 0.0" vertical offset spacing, against pattern 13, 0.1" triangle with 0.1" horizontal and 0.0" vertical offset spacing. This test evaluated the shape variable. No appreciable difference can be seen in image quality between the patterns. Similar spacing and pattern size appear to produce similar image quality results of the density gradients in this test.

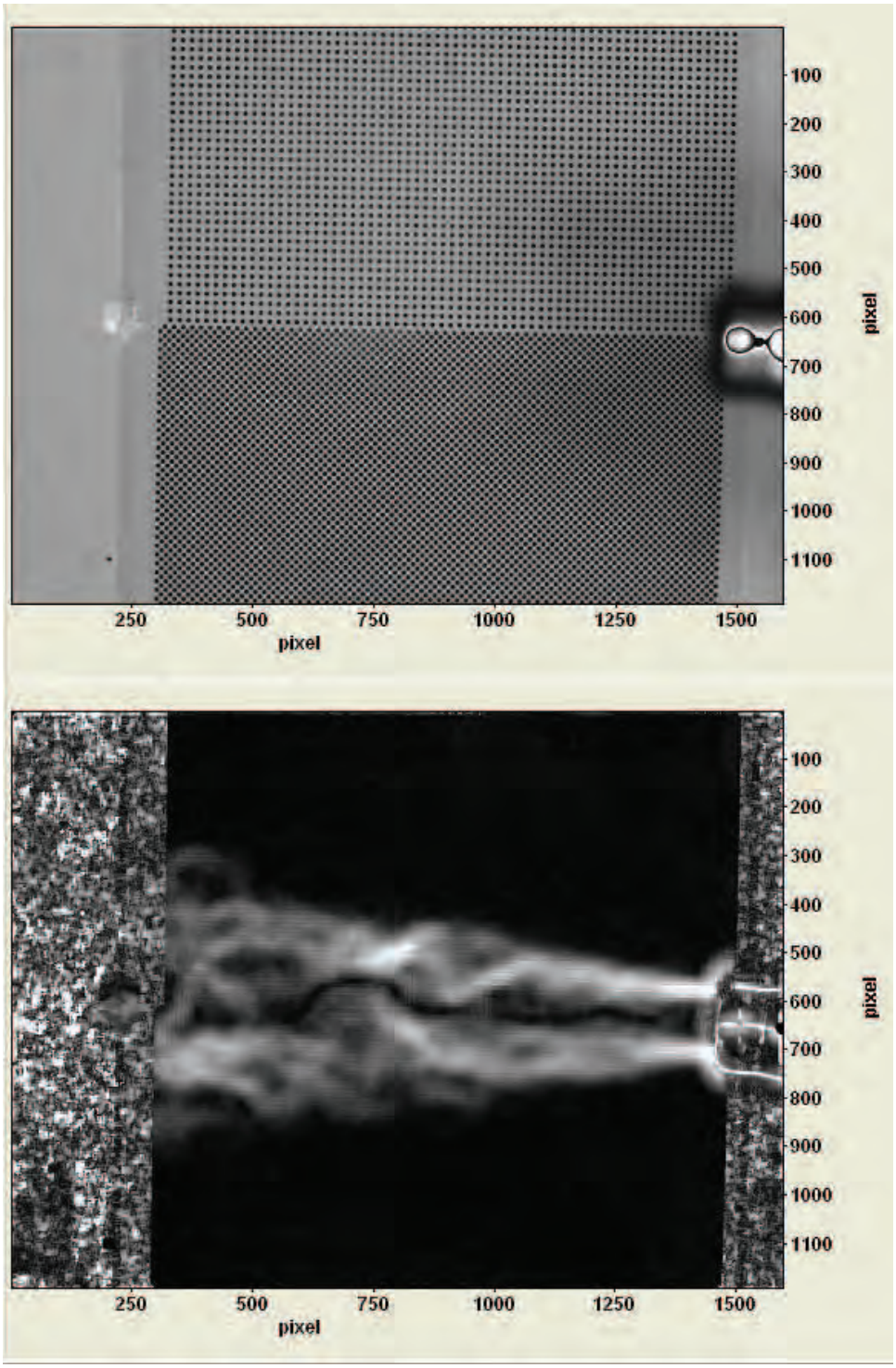

Figure 3.8: Test 11 using patterns 2 on bottom and 3 on top

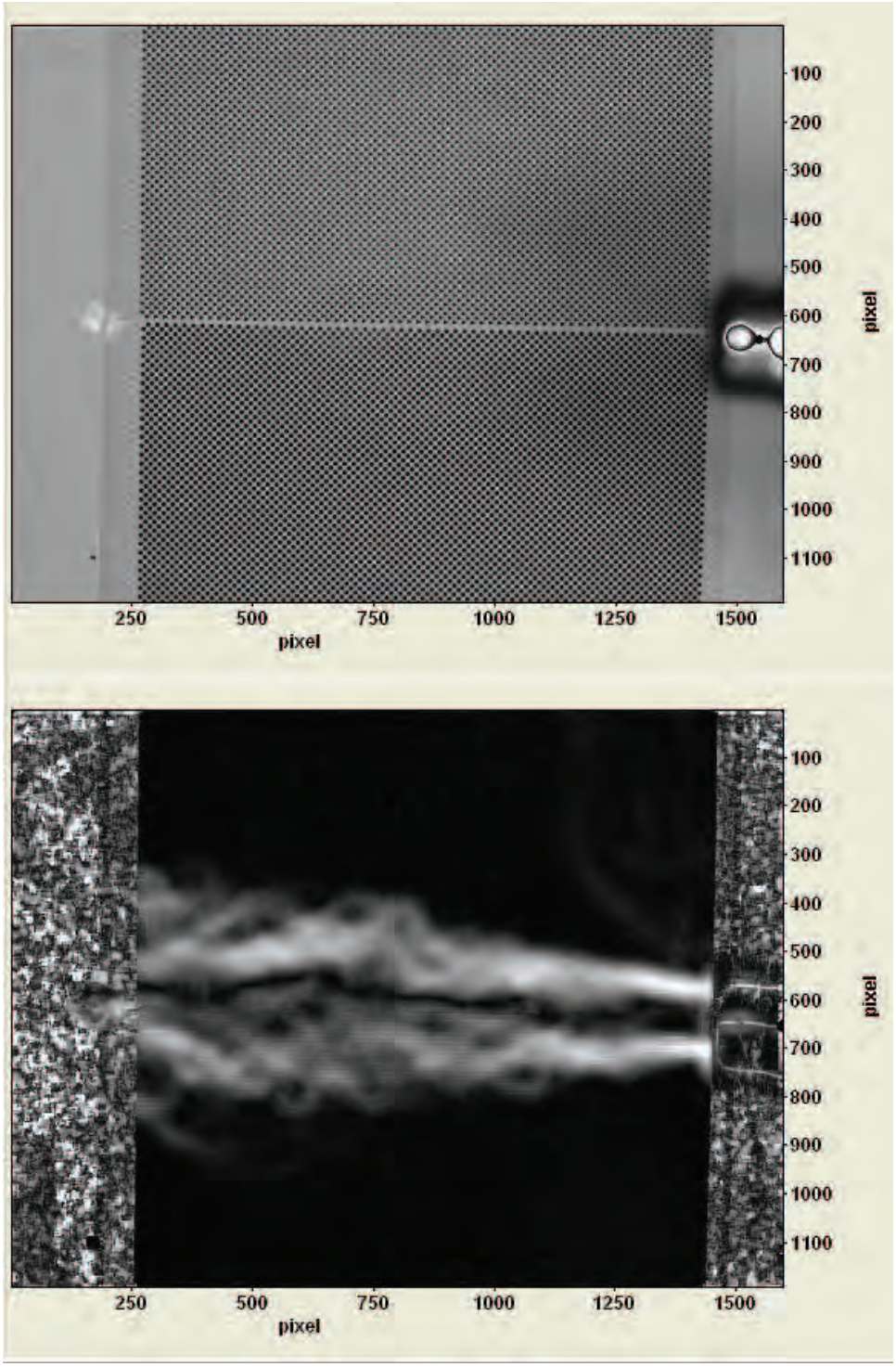

Figure 3.9: Test 12 using patterns 2 on bottom and 13 on top

There does appear to be more flow over the upper pattern seen in this test and some subsequent tests. This is believed to be non-symmetrical flow. Slightly more flow moving through the upper section of the heat gun nozzle as opposed to the lower section of the nozzle. When you zoom into the flow, similar detail can be seen in both patterns.

Fig. 3.10 compares pattern 2, 0.1" dot with 0.1" horizontal and 0.0" vertical offset spacing, against pattern 17, 0.1" hexagon with 0.1" horizontal and 0.0" vertical offset spacing. This test evaluated the shape variable. No appreciable difference can be seen in image quality between the patterns. Similar spacing and pattern size appear to produce similar image quality results of the density gradients in this test. Similar to test 12, the flow over the upper pattern appears to have slightly higher volume when compared to the lower portion, but both patterns reveal similar quality when you zoom in.

Fig. 3.11 compares pattern 3, 0.1" dot with 0.1" horizontal and 0.1" vertical spacing, against pattern 14, 0.1" triangle with 0.1" horizontal and 0.1" vertical spacing. This test evaluated the shape variable. No appreciable difference can be seen in image quality between the patterns. Similar spacing and pattern size appear to produce similar image quality results of the density gradients in this test.

Fig. 3.12 compares pattern 3, 0.1" dot with 0.1" horizontal and 0.1" vertical spacing, against pattern 20, 0.1" square with 0.1" horizontal and 0.1" vertical spacing. This test evaluated the shape variable. No appreciable difference can be seen in image

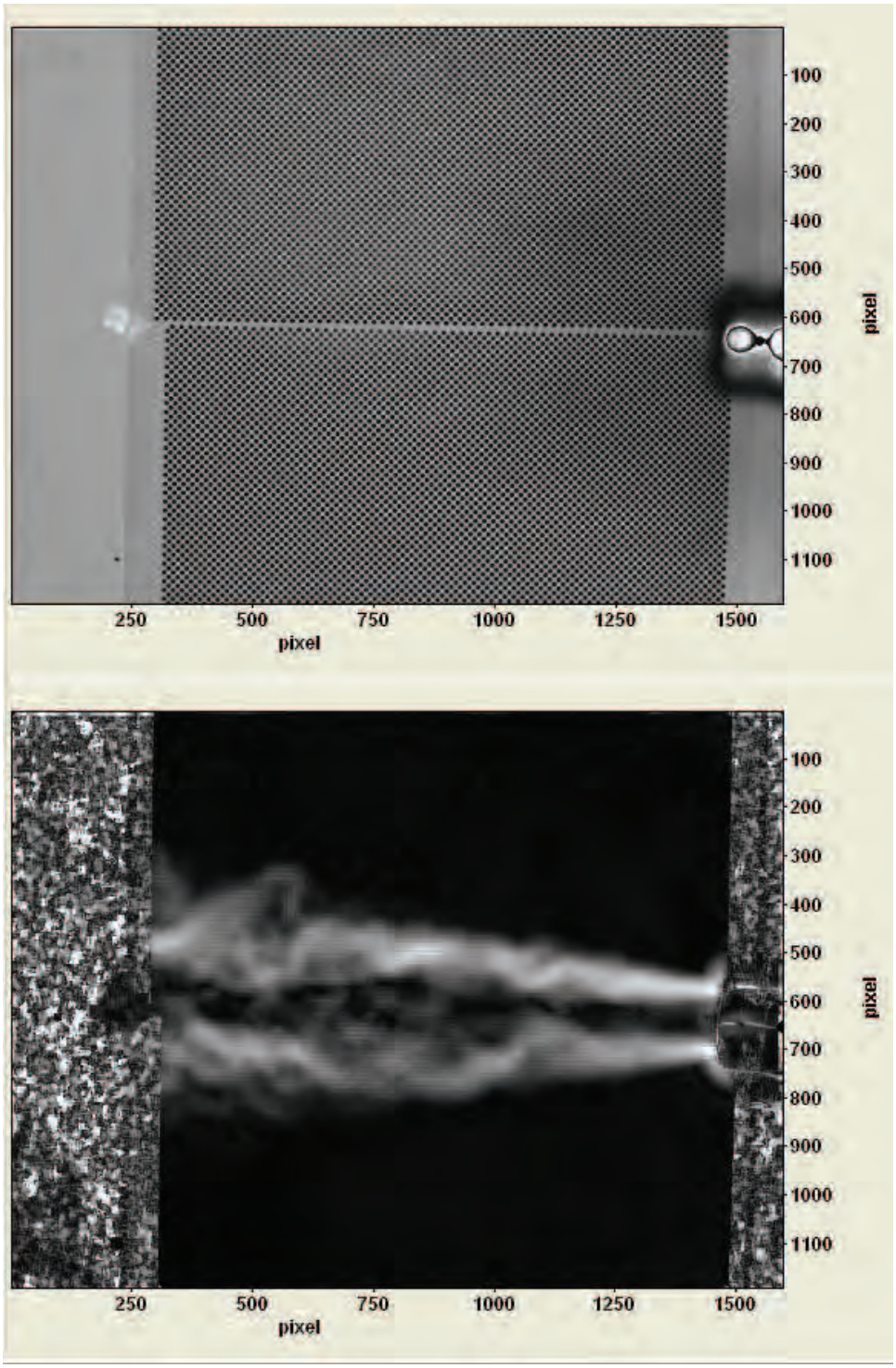

Figure 3.10: Test 13 using patterns 2 on bottom and 17 on top

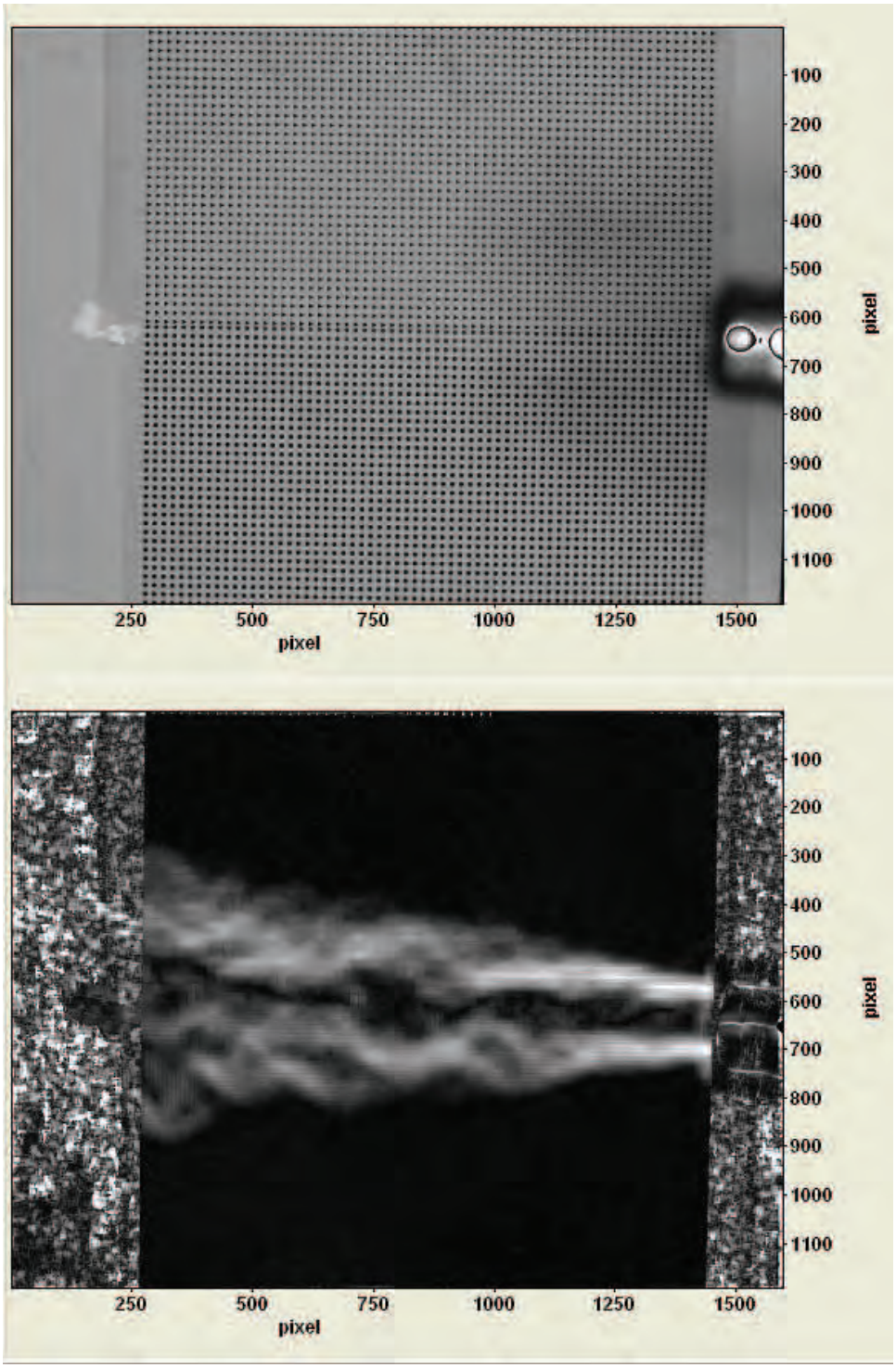

Figure 3.11: Test 14 using patterns 3 on bottom and 14 on top

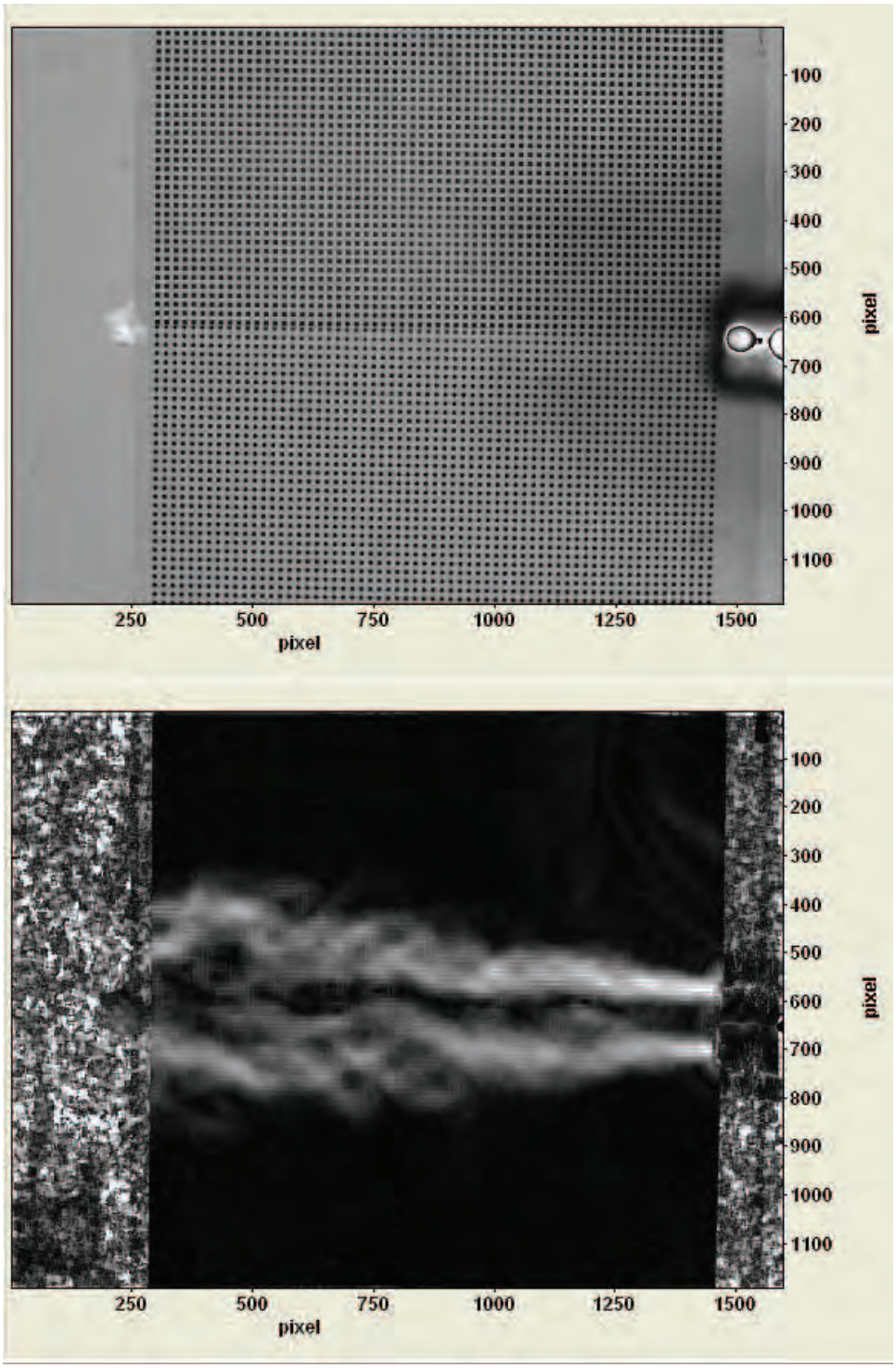

Figure 3.12: Test 15 using patterns 3 on bottom and 20 on top

quality between the patterns. Similar spacing and pattern size appear to produce similar image quality results of the density gradients in this test.

Fig. 3.13 compares pattern 3, 0.1" dot with 0.1" horizontal and 0.1" vertical spacing, against pattern 18, 0.1" hexagon with 0.1" horizontal and 0.1" vertical spacing. This test evaluated the shape variable. No appreciable difference can be seen in image quality between the patterns. Similar spacing and pattern size appear to produce similar image quality results of the density gradients in this test.

Fig. 3.14 compares pattern 4, 0.2" dot with 0.2" horizontal and 0.2" vertical spacing, against pattern 15, 0.2" triangle with 0.2" horizontal and 0.2" vertical spacing. This test evaluated the shape variable. No appreciable difference can be seen in image quality between the patterns. Similar spacing and pattern size appear to produce similar image quality results of the density gradients in this test.

Fig. 3.15 compares pattern 4, 0.2" dot with 0.2" horizontal and 0.2" vertical spacing, against pattern 21, 0.2" square with 0.2" horizontal and 0.2" vertical spacing. This test evaluated the shape variable. No appreciable difference can be seen in image quality between the patterns. Similar spacing and pattern size appear to produce similar image quality results of the density gradients in this test.

Fig. 3.16 compares pattern 4, 0.2" dot with 0.2" horizontal and 0.2" vertical spacing, against pattern 19, 0.2" hexagon with 0.2" horizontal and 0.2" vertical spacing. This test evaluated the shape variable. No appreciable difference can be seen

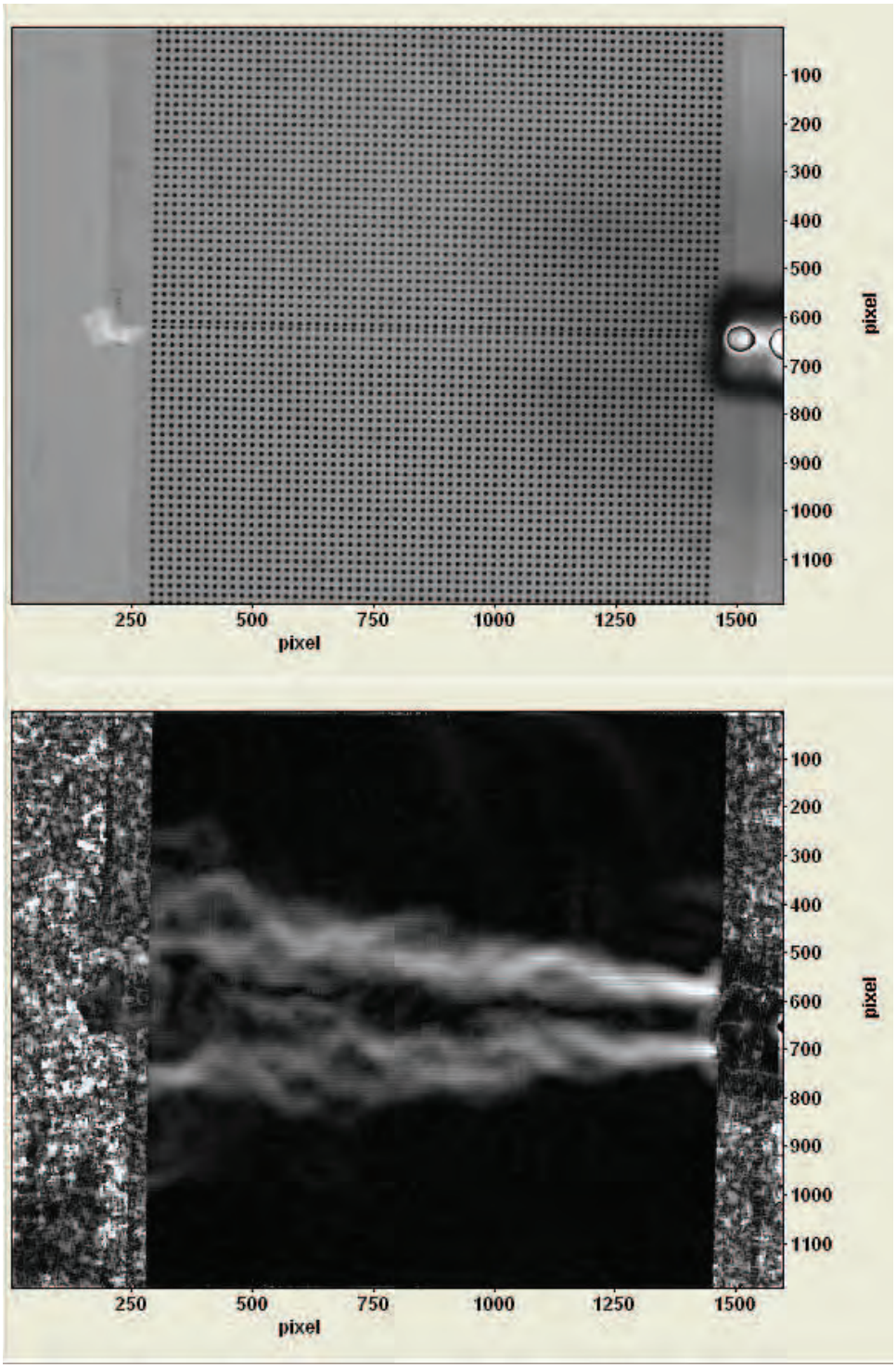

Figure 3.13: Test 16 using patterns 3 on bottom and 18 on top

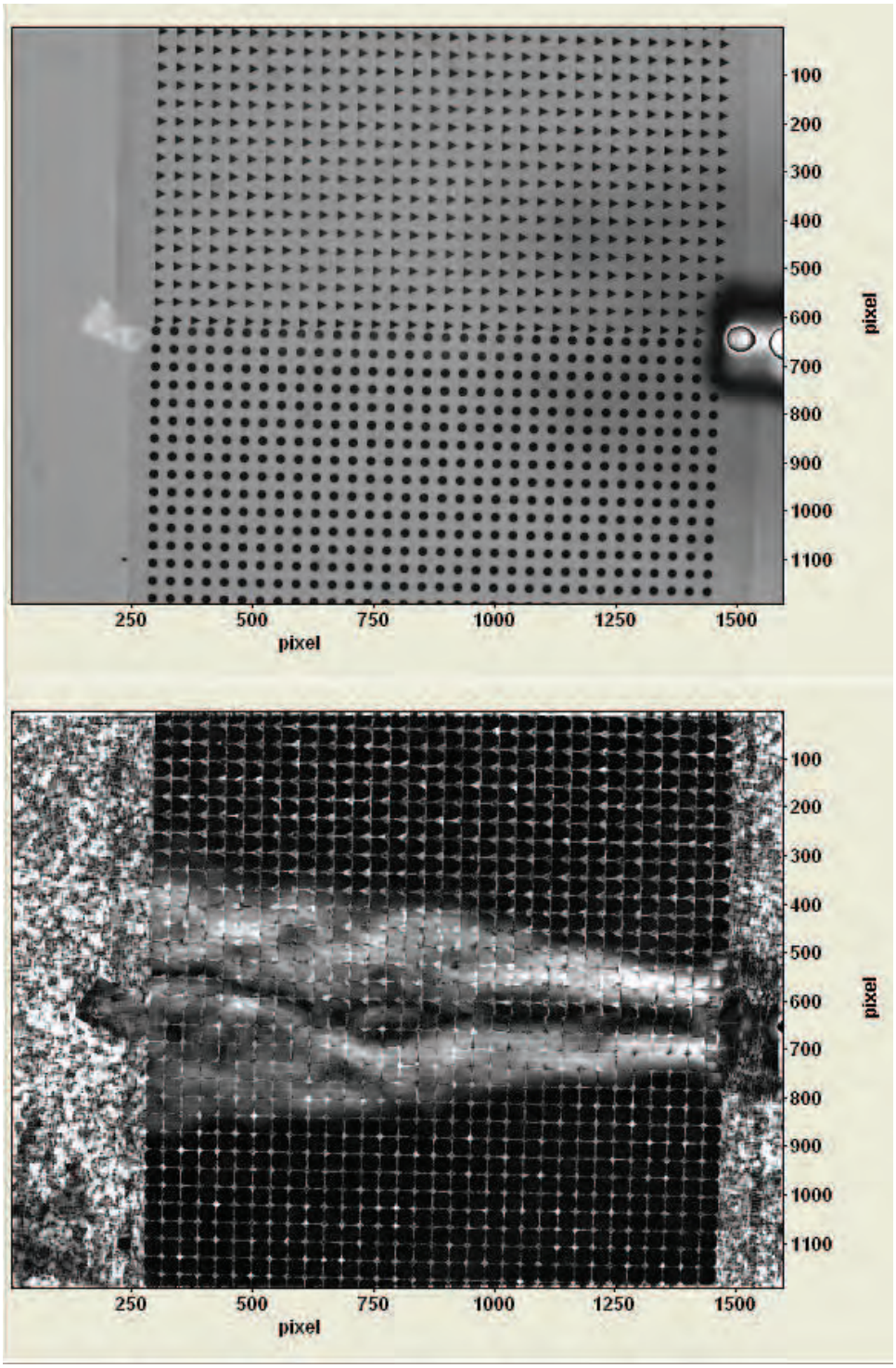

Figure 3.14: Test 17 using patterns 4 on bottom and 15 on top

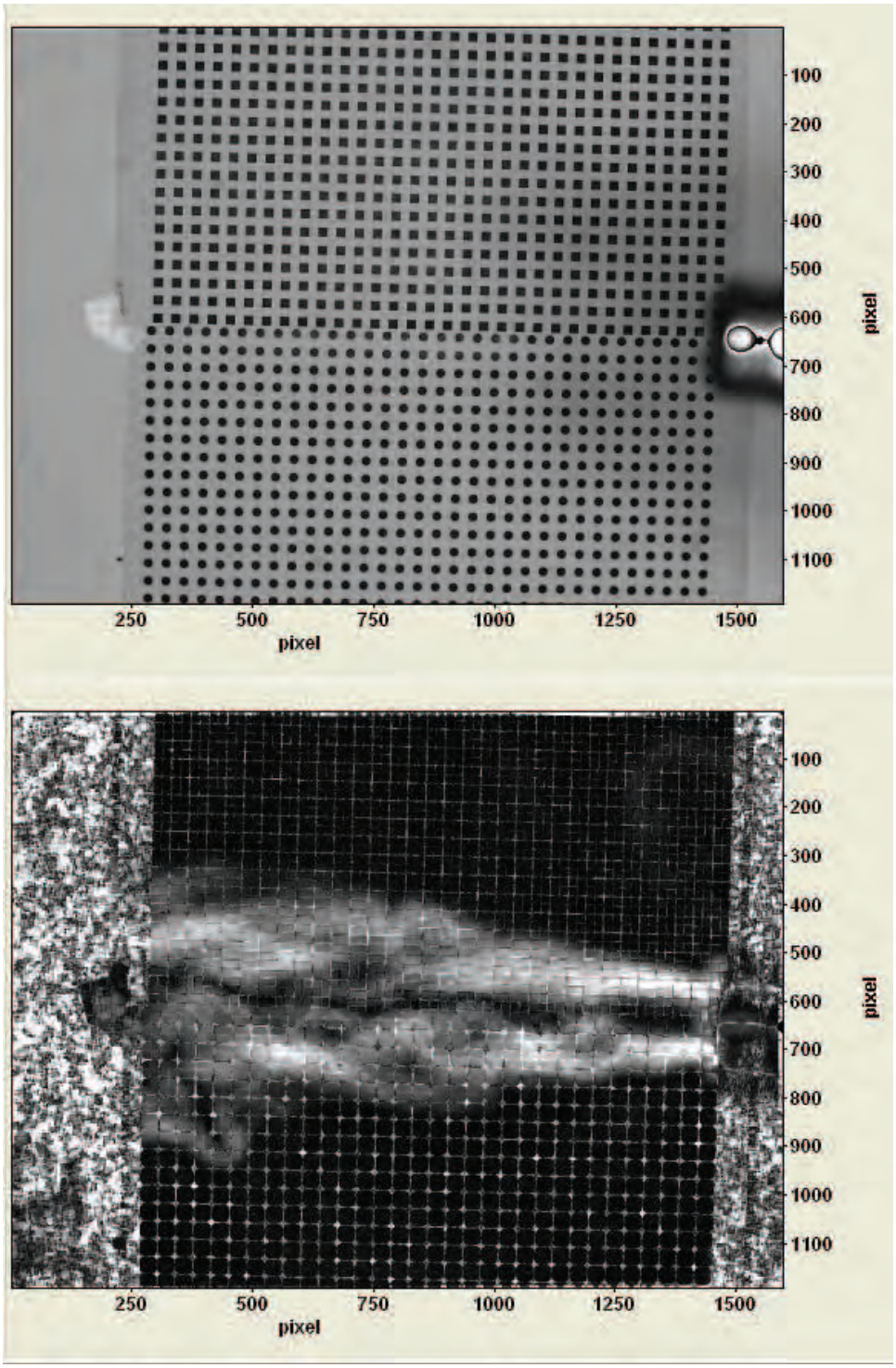

Figure 3.15: Test 18 using patterns 4 on bottom and 21 on top

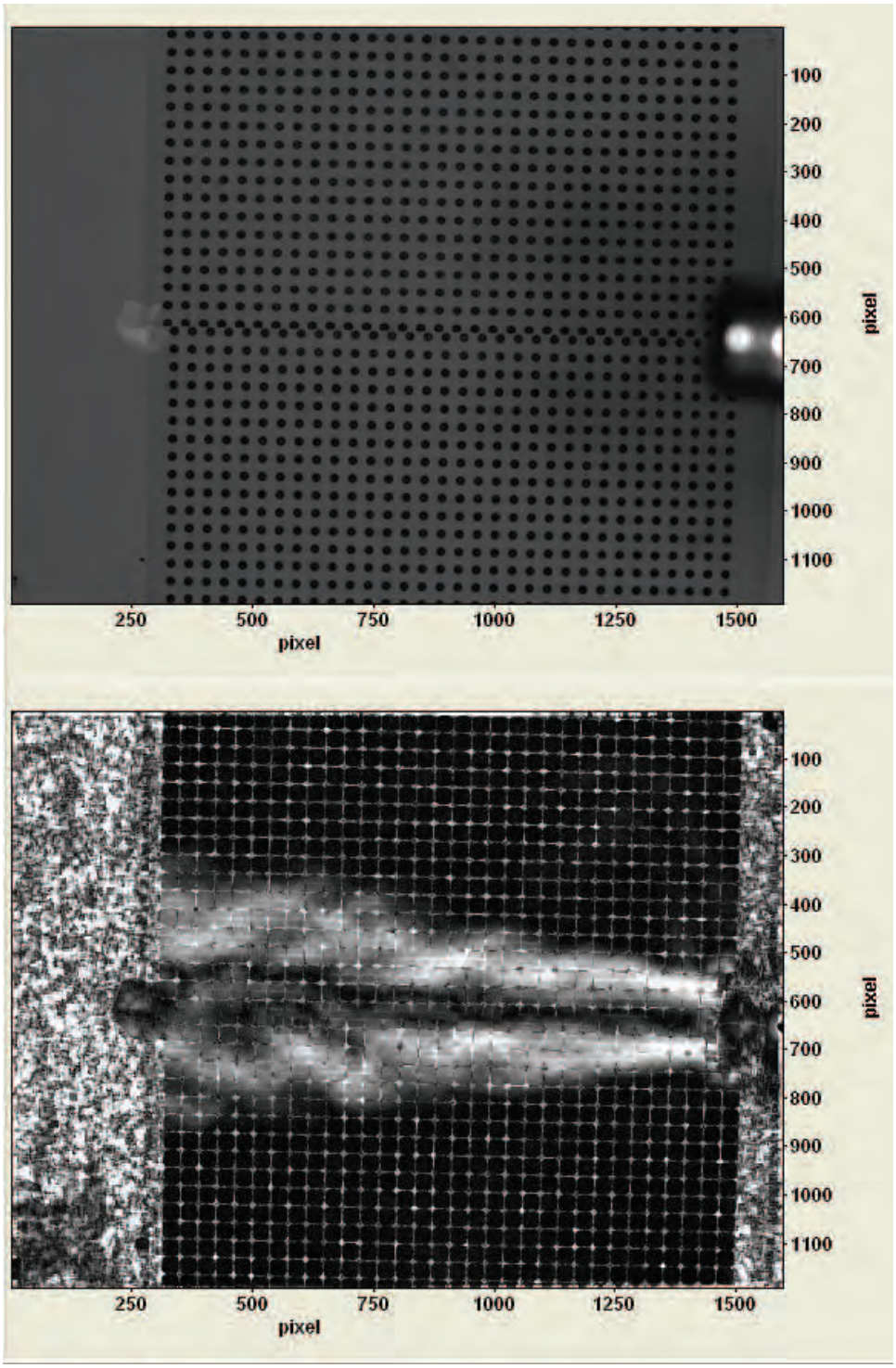

Figure 3.16: Test 19 using patterns 4 on bottom and 19 on top

in image quality between the patterns. Similar spacing and pattern size appear to produce similar image quality results of the density gradients in this test.

Fig. 3.17 compares pattern 5, 0.05" dot with 0.05" horizontal and 0.05" vertical spacing, against pattern 6, 0.05" dot with 0.05" horizontal and 0.0" vertical offset spacing. This test evaluated the spacing variable. This test revealed no appreciable difference in image quality between the patterns. Reduced spacing in pattern 6 did not increase image quality. Reduction in spacing smaller than pattern 5 at this distance does not increase sensitivity significantly.

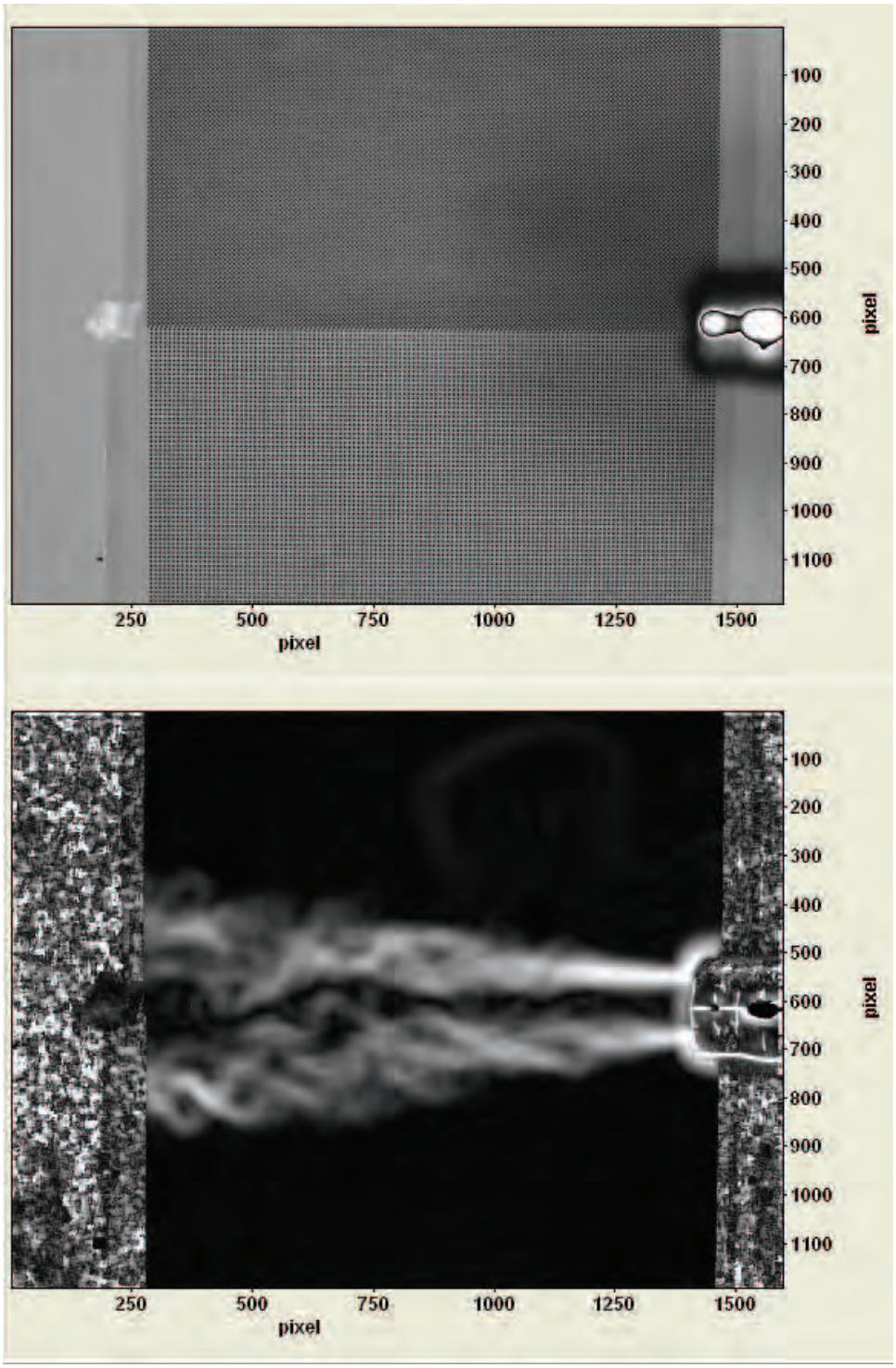

Figure 3.17: Test 20 using patterns 5 on bottom and 6 on top

Fig. 3.18 compares pattern 5, 0.05" dot with 0.05" horizontal and 0.05" vertical spacing, against pattern 3, 0.1" dot with 0.1" horizontal and 0.1" vertical spacing. This test evaluated the size and spacing variables. Pattern 5, the lower pattern with smaller pattern size and spacing, provided better imaging quality. Dot size and spacing above pattern 5, or 0.05", produces decreased image quality.

Fig. 3.19 compares pattern 6, 0.05" dot with 0.05" horizontal and 0.0" vertical offset spacing, against pattern 2, 0.1" dot with 0.1" horizontal and 0.0" vertical offset spacing. This test evaluated the size and spacing variables. Pattern 6, the lower pattern with smaller pattern size and spacing, provided better imaging quality. Again, as in test 21, this confirms that pattern and spacing size above 0.05" decreases image quality. The changes in image quality are minimal, but when zooming in, increased image quality is very noticeable.

Fig. 3.20 compares pattern 7, 0.3" dot with 0.3" horizontal and 0.0" vertical offset spacing, against pattern 8, 0.3" dot with 0.3" horizontal and 0.3" vertical spacing. This test evaluated the spacing variable. Pattern 7, the lower pattern with smaller spacing, provided better imaging quality. Image quality was still poor if compared to results of even smaller spacing such as in test 22.

Fig. 3.21 compares pattern 9, 0.5" dot with 0.5" horizontal and 0.0" vertical offset spacing, against pattern 10, 0.5" dot with 0.5" horizontal and 0.5" vertical spacing. This test evaluated the spacing variable. Pattern 9, the lower pattern with smaller spacing, provided slightly better imaging quality. The results of this test are

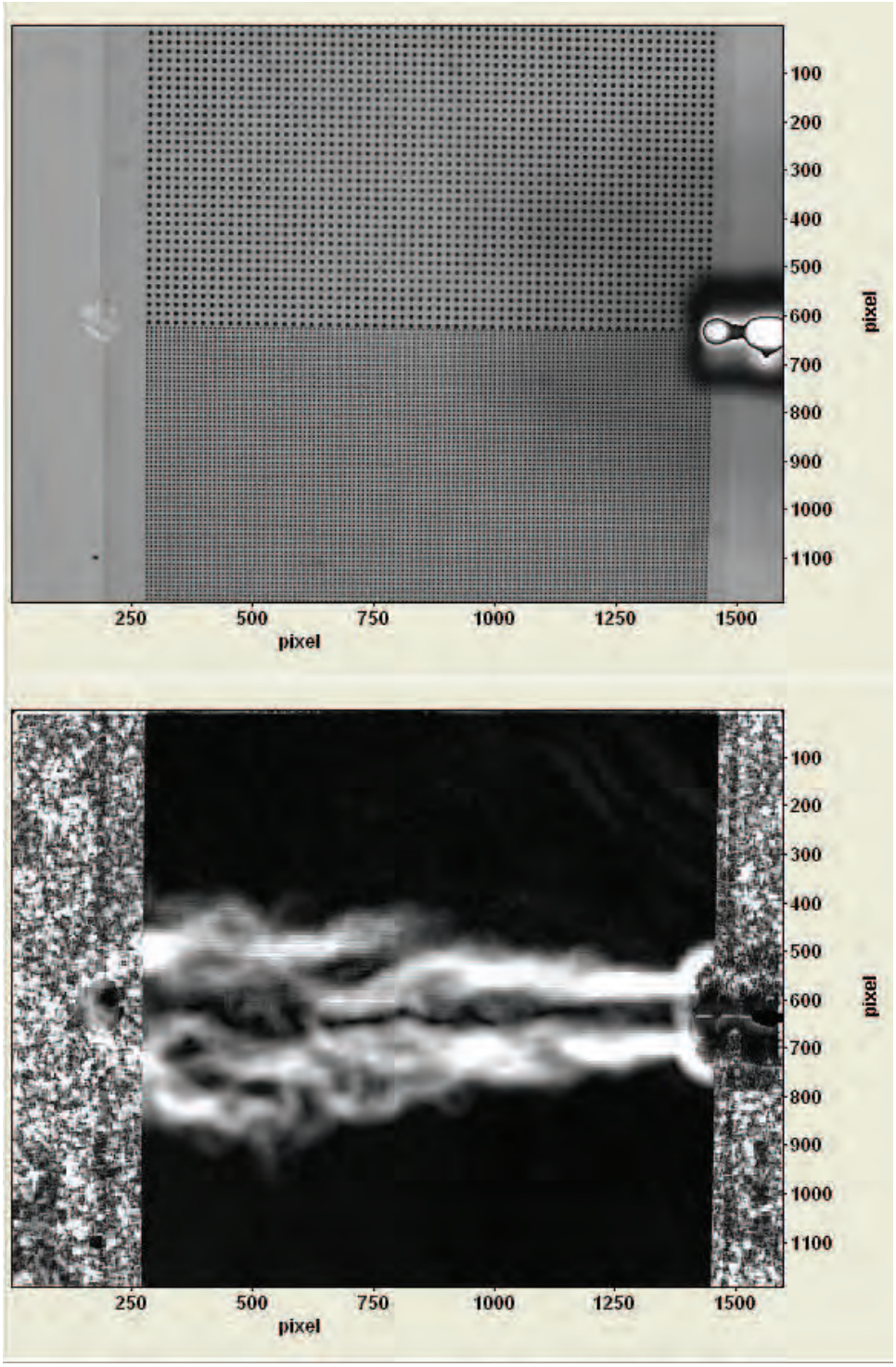

Figure 3.18: Test 21 using patterns 5 on bottom and 3 on top

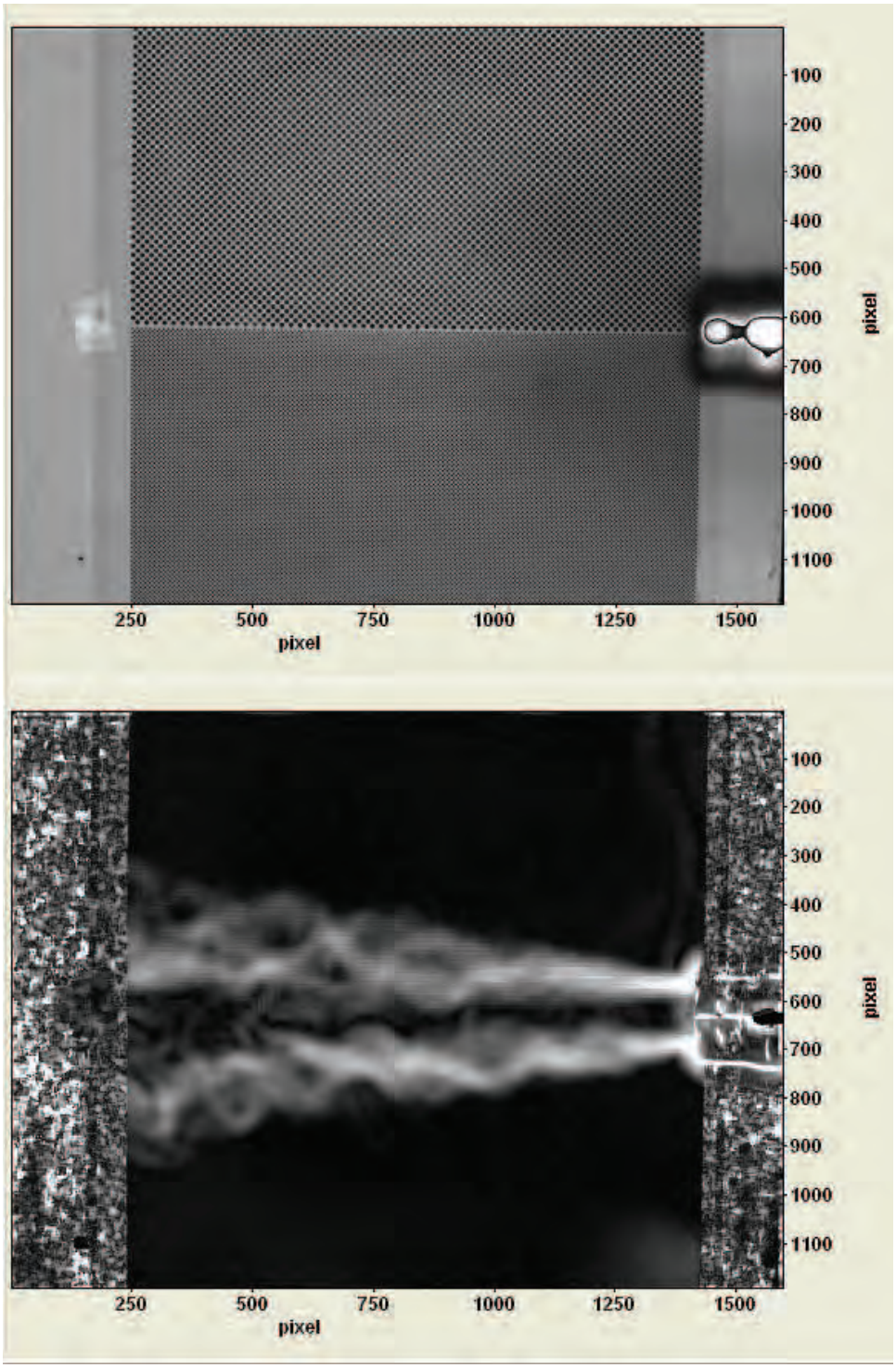

Figure 3.19: Test 22 using patterns 6 on bottom and 2 on top

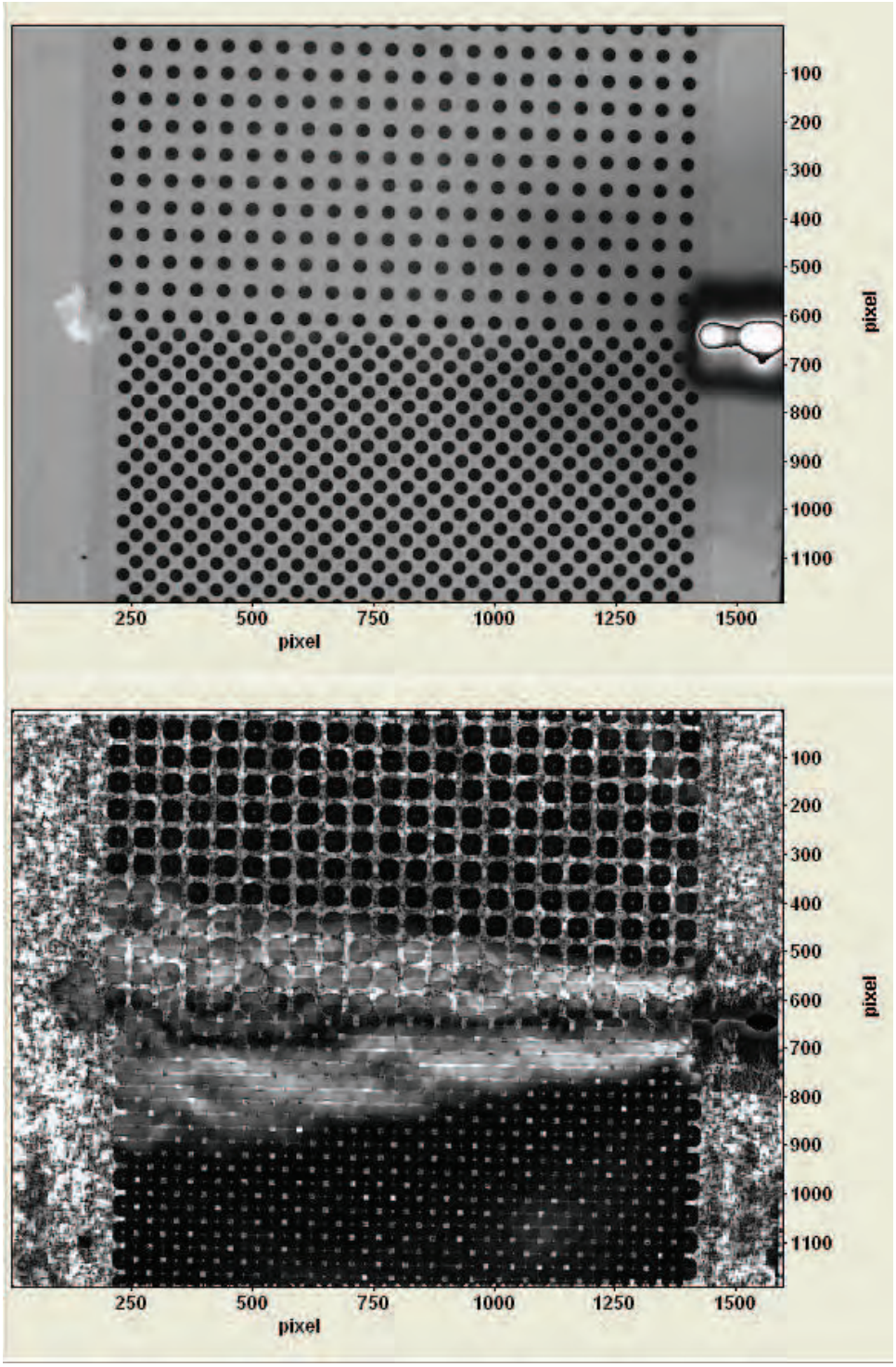

Figure 3.20: Test 23 using patterns 7 on bottom and 8 on top

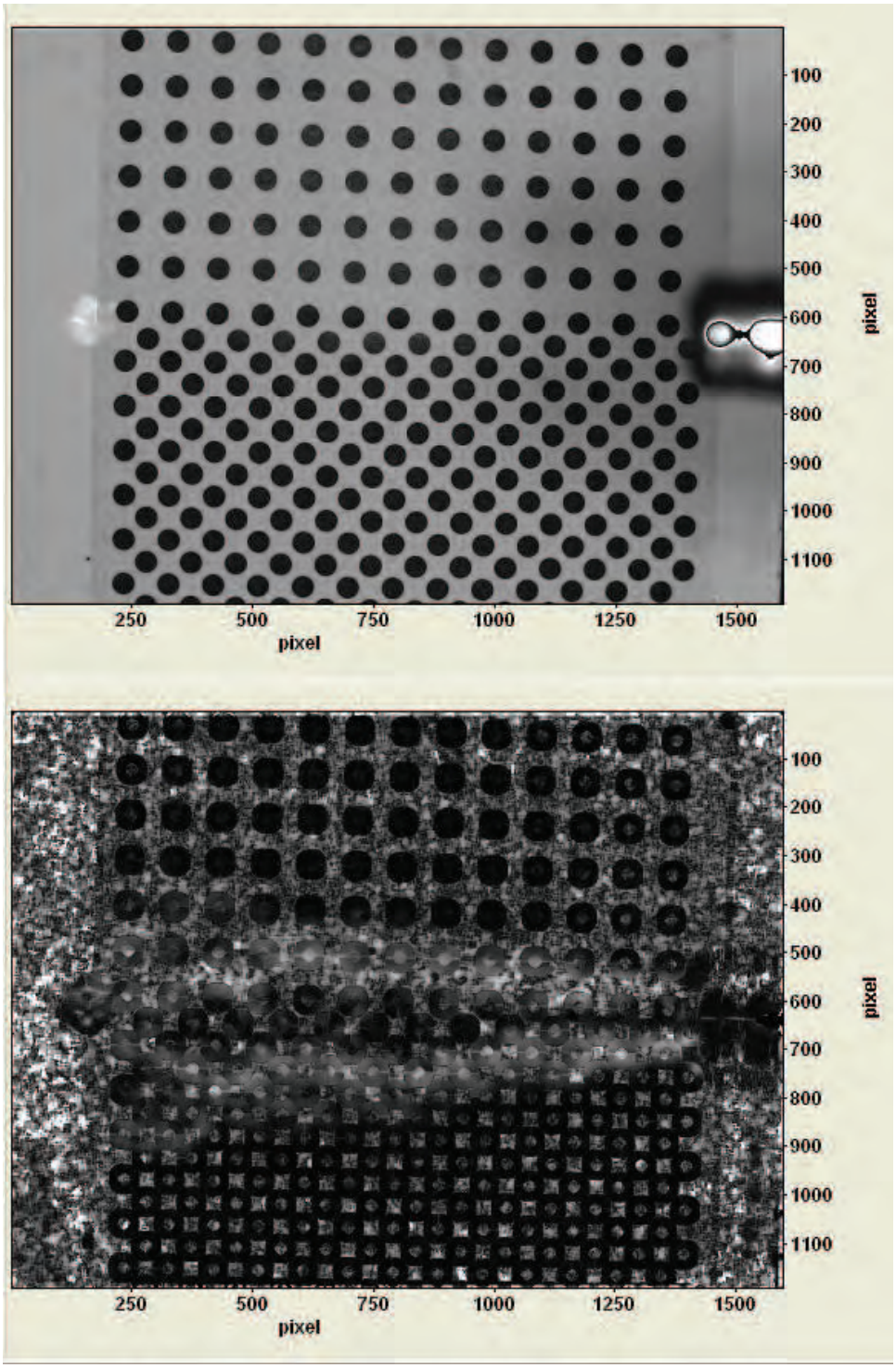

Figure 3.21: Test 24 using patterns 9 on bottom and 10 on top

very similar and the change in size of relatively large dots and spacing is difficult to discern. When you zoom into the image you are able to see slightly better image quality in pattern 9.

Fig. 3.22 was a test using alternate background painting methods. Instead of using printed patterns on paper, this test used metal plates stamped with dot patterns as a template to spray paint patterns onto a board. This test compares plate 1, 0.18" dot with 0.12" to 0.25" spacing, against plate 2, 0.12" dot with 0.06" to 0.18" spacing. Plate 2, the upper plate with smaller spacing and pattern size, provided better image quality. This test has a noticeable increase in the field of view. Magnification was reduced and the amount of background increased to approximately 2.5 ft square. The decrease in focal length does prevent from comparing the size and spacing results of this background to previous tests, but comparisons between the two plates can still be made. This test is discussed in more detail in the next section.

3.3 Additional Background Testing Results

Beyond the standard test matrix that was setup with prepared background patterns, additional patterns were available in the lab for use. Test 25 was an additional test carried out on a background sprayed on to a foam backer board through metal plate templates as seen in Fig. 3.23. The metal plates were stamped with dot patterns. Plate 1 has 3/16" holes with 1/8" to 1/4" varied spacing. Plate 2 has 1/8" holes with 1/16" to 3/16" varied spacing. Plate 2 with smaller dots and spacing is located at the top of the background. The plates are rotated on the second spray pass

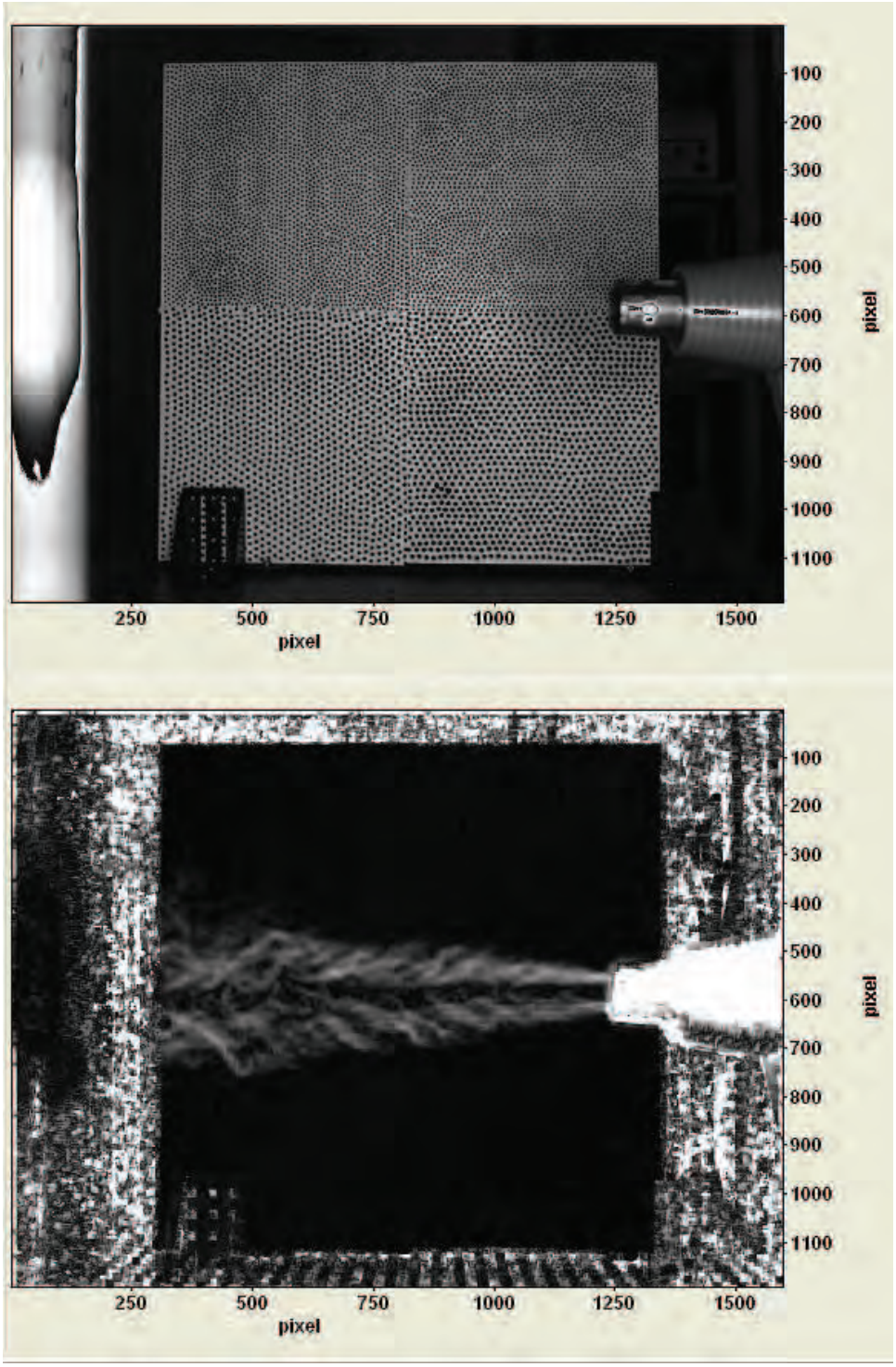

Figure 3.22: Test 25 using plate 1 on bottom and plate 2 on top

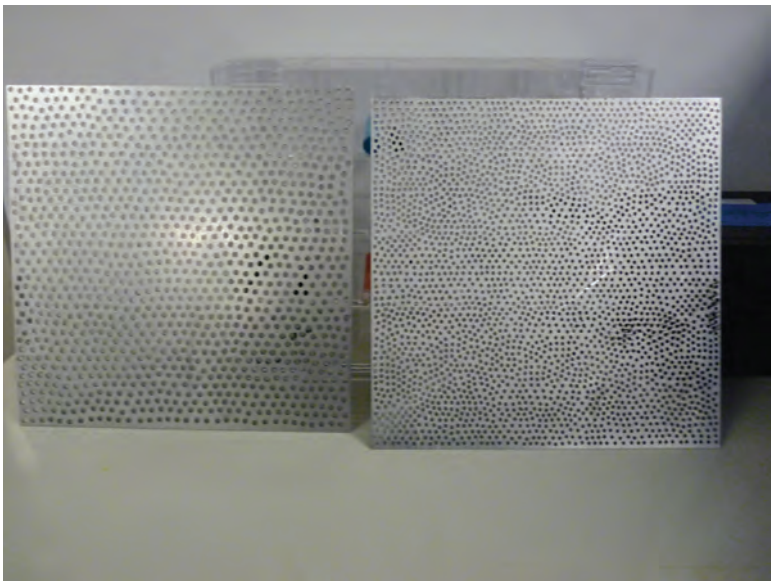

Figure 3.23: Stamped metal plates for spray on background patterns

horizontally across the background to mix up the pattern alignment. This was also a test of how well the application of dot patterns could be applied through a spray on template.

The spray painting of the dot pattern through the fine mesh plate was problematic. Full contact with the plate to the foam board was difficult. When contact was lost in areas, due to bowing of the plate, over spray occurred on the foam board, between the metal plate and board. For a fine mesh pattern like this, it made the edges of the dot pattern less defined. This is thought to contribute to poorer images due to the software being less likely to define shifting of the dot edges between images. Depending on the scale of the experiment, an even finer dot pattern may be desired. For instance, if the area of interest of the density gradient is very small, then we would prefer to zoom in on this area and have a background dot pattern that is small enough in size to allow for changes in contrast within only a few pixel

range. Application of this type of pattern with very small dots would have proved to be even more difficult to apply through the use of paint spray. Patterns this small would typically need to be created through the use of a printing technique. Patterns can be generated through pseudo random methods with algorithms in MATLAB® then printed with modern office or shop printers onto whatever backing material is desired. This, of course, then brings into question how the printed background will be applied behind the test object. In a lab environment, application could possibly be done very easily, similar to this thesis on a poster board, or it could be placed behind a transparent panel if necessary.

For applications in larger industrial settings such are large scale wind tunnels, this becomes a more difficult problem. In Reinholtz's application of a background in a large scale wind tunnel [7], the area of interest was large enough that a dot pattern could be painted onto the test cell walls relatively easily. But, even if the scale is large enough to permit hand painting of the background on the tunnel wall, there are almost always objects within the tunnel that need to be negotiated. An example would be the porosity holes of a transonic test section wall as seen in Fig. 3.24. Obstacles such as these, and others throughout a test cell, can prove difficult for any type of pattern application. If painting of the background proved too difficult, a printed background on adhesive paper could be used. Use of an adhesive paper on the walls could create other issues such as delamination under high speed conditions.

Whatever method is used to apply the background, it is always preferred to place it on the tunnel wall. Removing sections of the tunnel wall to add transparent

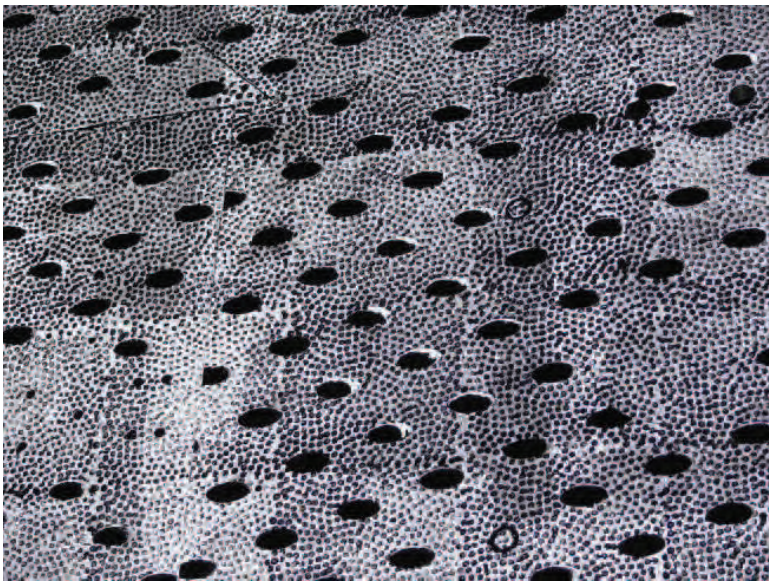

Figure 3.24: Transonic test section wall with porosity holes and painted BOS background [7]

sections is problematic. In a transonic test section this will cause changes in the porosity. Also, this defeats the purpose of using a new technique such as BOS. Using a BOS system instead of a classical schlieren system allows you to get rid of large optical access viewing areas. Bringing back the requirement for a large transparent background area makes the use of BOS much less desirable.

Results of test 25 and its pseudo random dot pattern show similar results to previous tests. The smaller dot pattern on the upper half imaged slightly better than the larger dot pattern shown on the bottom half of the background. Results of test 25 can be seen in Fig. 3.25. The resolution of the flow as it passes over the background patterns shows clearer imaging over the smaller dot pattern. This is difficult to see at normal magnification, but becomes more apparent as you zoom into the image.

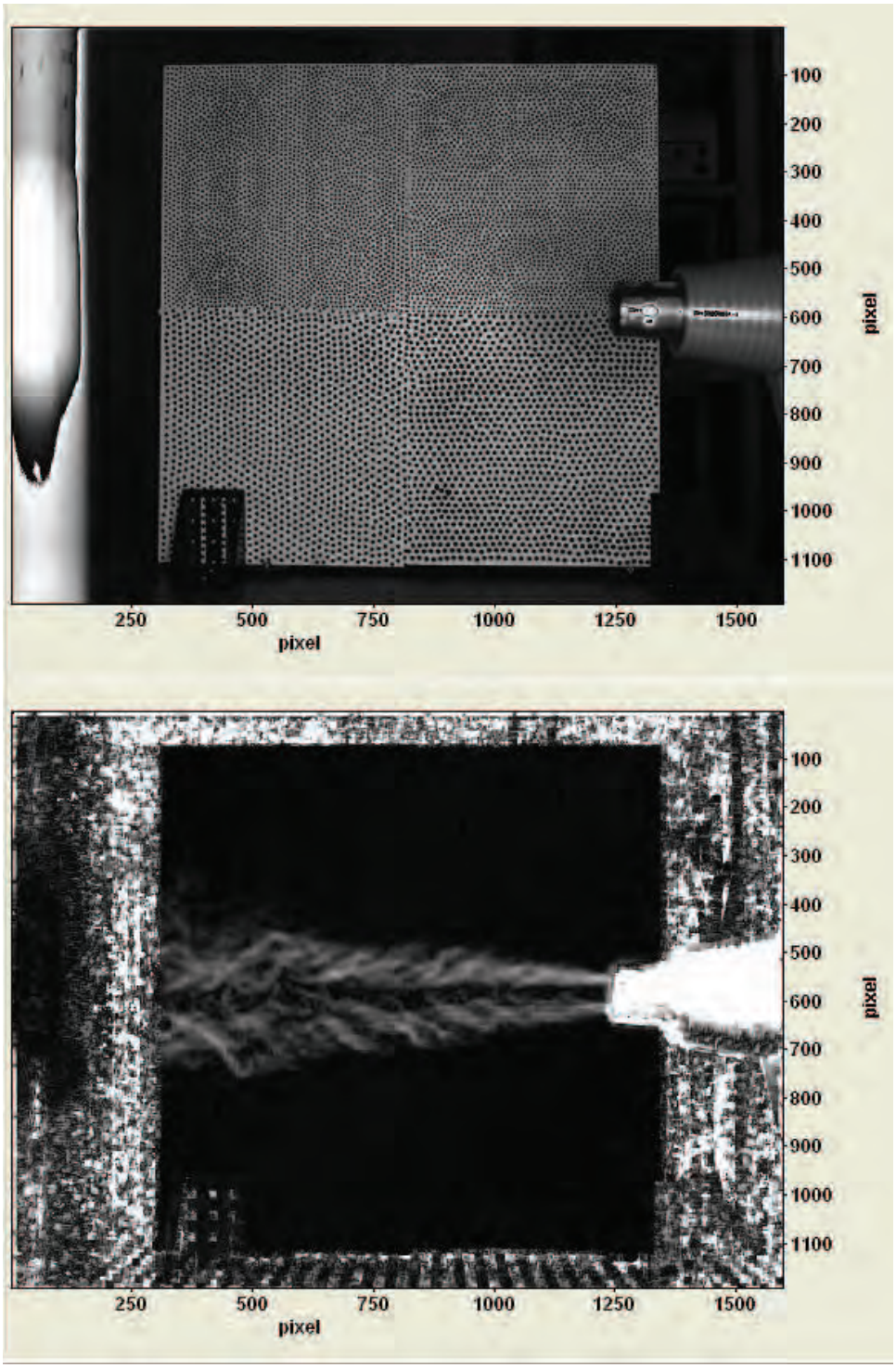

Figure 3.25: Test series 25 with stamped metal plate pseudo random dot patterns

A significant change in test 25 should be noted. The subject area, or density gradient area of interest, was enlarged. This is readily apparent by noting the amount of background that is now visible when compared to previous tests. During this test, a background of approximately 3′ wide is visible. This increase in field of view now allows for the depth of focus to include both the background and density gradient. Notice the heat gun is now in focus along with the background. This decrease in magnification of the air flow area of interest results in an effective decrease in focal length. This increases the size and spacing of the background dot pattern required for system sensitivity. Even though field of view was increased on this test, the comparison between dot patterns can still be made effectively.

To estimate the expected optimal dot size for this test geometry we use the 3′ background width along with the 1600 pixel width in Eq. 3.1.

$$3' = 36" \div 1600\, pixels \approx 0.053\, inch\, per\, pixel \times 3\, pixel\, recommendation \approx 0.068" \tag{3.1}$$

This predicts an optimal dot size of approximately 0.07". The qualitative comparison of the two patterns showed an improvement in image quality with the smaller plate 2, 0.13", over plate 1, 0.19". This shows an improvement in image quality as we get nearer to the expected optimal sizing of 0.07".

Test 26, shown in Fig. 3.26, was an alternate test done to compare changing of contrasting colors between background and dot. Patterns with white dots on black

backgrounds were evaluated against patterns with black dots on white backgrounds. Note how the software processed the lower half of the flow with higher intensity when compared to the upper half. This is thought to be possibly due to a global shift of the background pattern between images. The camera or background may have shifted slightly in the vertical axis between images causing a net decrease in the upper half magnitudes along with a net increase in the lower half magnitudes. Even with the visual difference in magnitudes between upper and lower halves, evaluation of the flow as it passes horizontally over the vertical strips can be made.

Dot size for the patterns on test 26 were all similar except for the center pattern that had smaller dots with larger spacing. Approximate 6" vertical strips with changing size and color. Dot size is approximately 7/32" with average spacing except for the center section, which has 3/32" dots with large spacing. There is no discernable change in image quality between the white dots on black background and black dots on white background. This was expected as the contrast between the dots and spaces stays the same. This contrast is a key aspect in image quality. The center section with smaller dots and larger spacing did show poorer image quality. This was due to the dot size and spacing, as seen in previous tests, and not the dot color.

3.4 Supplemental Analysis of High Speed Video Imaging

Additional time stepped images, or video, was taken with the Phantom camera and are discussed in this section. This was beyond the original scope of the thesis, and are added as supplementary reporting. The availability of the high speed camera

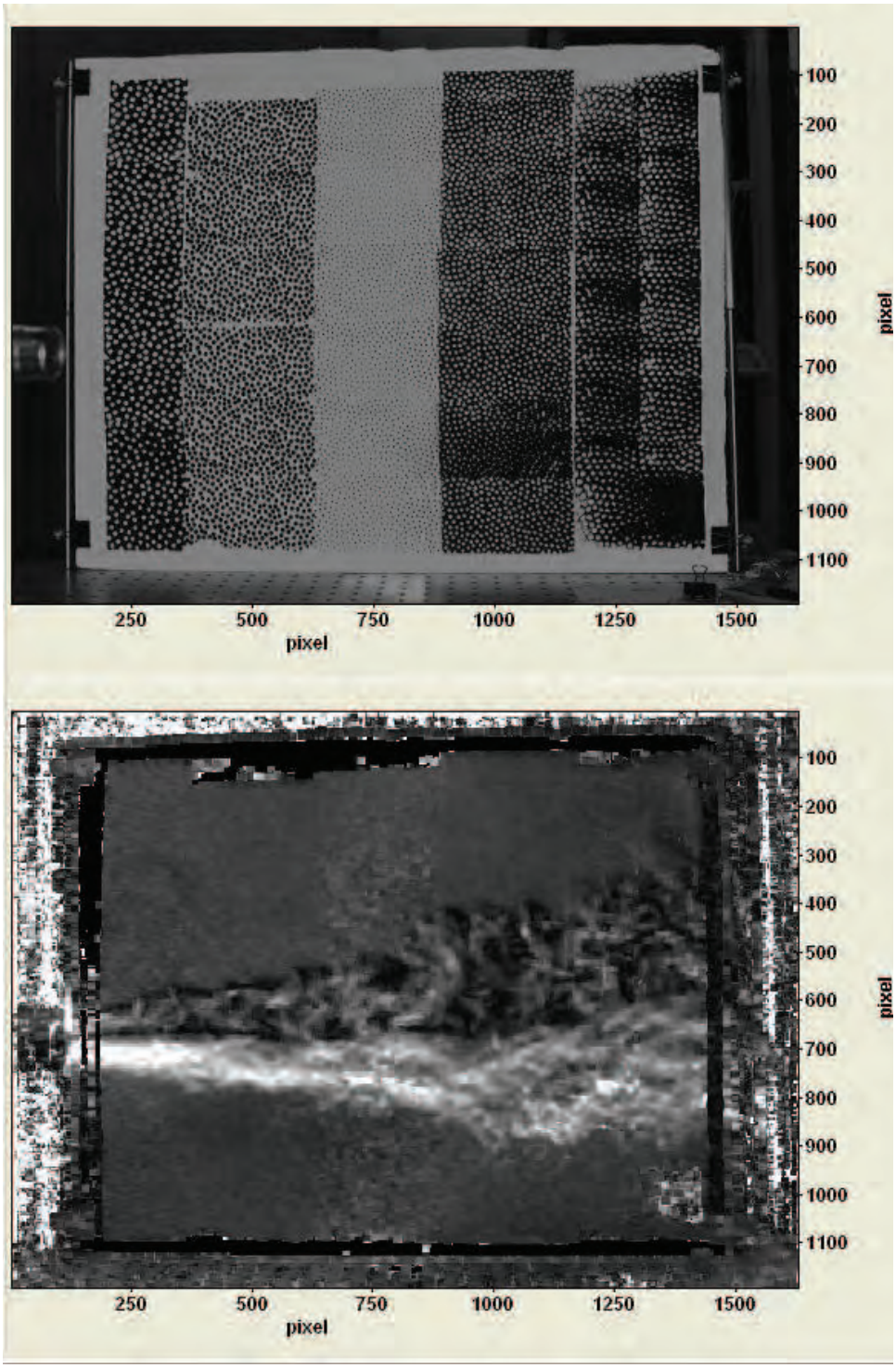

Figure 3.26: Test series 26 with pattern color contrast changes

presented the opportunity to take high speed video of the flow. Ideally it would have been prudent to take multiple time resolved images of all the tests and then do PIV style analysis on the BOS processed images to further scrutinize flow over the test dot patterns. Unfortunately this was not completed on each test series. Video image processing was not planned for inclusion in this thesis originally. The video was taken with a larger field of view to capture more of the flow, and was taken after the test series was complete to practice processing video imaging with the software. Had the video been planned for inclusion in this work early on, it would have been prudent to image the video in a similar geometric setup as the earlier tests with the optimal dot size.

One video series was captured on the background used in test 26. Three frames of this video are shown in succession in Fig. 3.27. These are BOS vector plots of the magnitude and direction of the dot displacement between two successive images. These changes in position of the dots on the background correspond to changes in the density gradient in the flow field. The vector plots of the changing gradients do little as an additional analysis tool beyond the previous BOS images shown in this thesis and used for qualitative analysis, but they do show grouping of the vectors well. This grouping of vectors represent structures in the flow. The structures in the flow, can be tracked through successive images. This can be seen as you scan down through the frames in Fig. 3.27.

To further analyze the flow of the captured time lapsed images, the use of schlieren PIV processing can be completed. The BOS images are processed normally

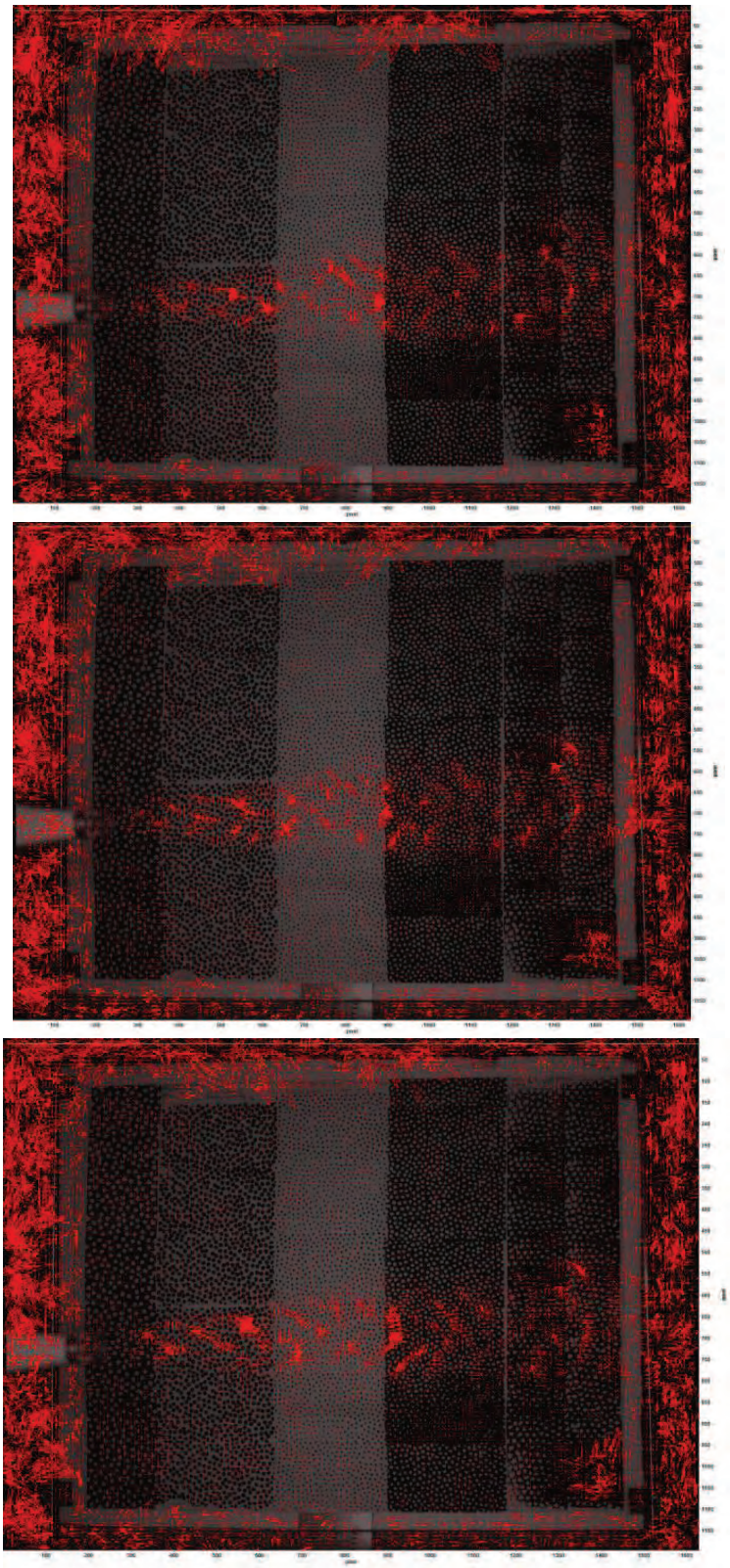

Figure 3.27: Three successive BOS analysis vector plot frames from video taken on same background as test 26

to produce the images previously seen in this thesis. Then, the successive images can be processed a second time by the PIV software to track position changes of identifiable structures in the flow. In the turbulent flow the software tracks the grouped vector structures from image to image. This change in position between frames can then be plotted as velocity vectors to further analyze the flow.

To manually estimate the velocity of the flow the eddies can be tracked manually between images. An example of this manual tracking is shown here. The heat gun used for the test was a Weller 6966C. Manufacturers specifications for the velocity exiting this model heat gun at the nozzle is approximately 5 miles per hour (mph). Flow in this unbounded free jet naturally slows as it moves to the right downstream. Distance traveled across the flow can be correlated to a known distance, such as the length of the nozzle tip on the heat gun. With a known distance traveled and the known frame rate time between images, the velocity of the flow can easily be estimated. The estimates taken at different parts of the flow correlated with the known heat gun velocity. The estimated flow velocity at the center left of the flow, the area of highest expected velocity, is shown in Eq. 3.2. The estimated velocity at the far right of the flow is shown in Eq. 3.3.

$$\frac{displacement\ of\ structure}{time\ between\ images} \approx \frac{0.25\ in}{0.002\ s} \approx 7\ mph \tag{3.2}$$

$$\frac{displacement\ of\ structure}{time\ between\ images} \approx \frac{0.1\ in}{0.002\ s} \approx 3\ mph \tag{3.3}$$

Secondary PIV processing produces velocity vectors showing the magnitude and direction of the change in position of the structures within the flow from one time lapsed image to the next. The pixel length can easily be correlated to the size of a known feature in the background or target cross section. The video was taken at 500 frames per second. With a known length of pixel shift and time between images, velocity of the jet can easily be calculated.

To further visualize the flow, a group of the velocity mapped images can be averaged and imaged together. A sample of 100 time lapsed images were processed for velocity mapping. These velocity maps were averaged and mapped in Fig. 3.28 and Fig. 3.29. The software quantifies the position change into pixel shift. Both figures list scales in length of pixel shift. Fig. 3.28 maps velocity with an intensity map that shows color intensity of the amount of pixel shifts within the regions of the flow. This figure averaged position shift in the horizontal direction only and shows the color scale on the right side. Fig. 3.29 has a scale in the upper left corner that corresponds to pixel shift. This figure averaged the position change in the horizontal and vertical. The figure has 3 images, with the 2nd and 3rd images showing magnified regions of the same flow. The averaged vector arrows flow primarily to the right in the middle section while angling upward at the top edge and downward at the bottom edge as the flow disperses to the right. This corresponds well to the known properties of the flow. More simply put, Fig. 3.28 corresponds to the simple Eq. 3.4. Where $\bar{v}_x$ is the average flow velocity in the horizontal direction, $d\bar{x}_x$ is the average horizontal displacement of the flow and $d\bar{t}$ is the average time between image pairs, all over the

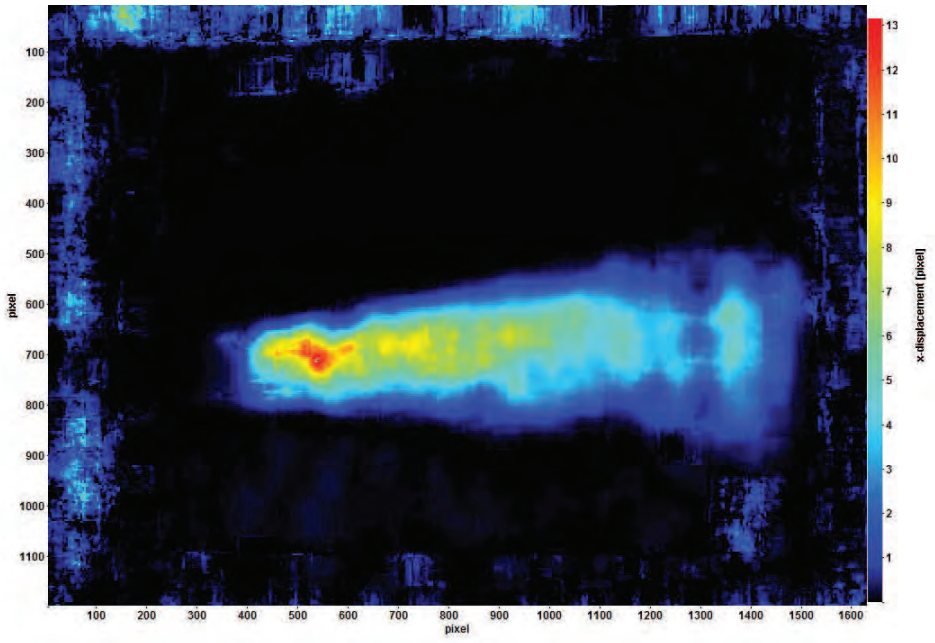

Figure 3.28: Intensity map of velocity vector magnitudes in horizontal direction

100 processed frames. Put another way, $\bar{v}_x$ is the average horizontal displacement of the tracked structures in the flow with respect to the average time between frames.

$$\bar{v}_x = \frac{d\bar{x}_x}{d\bar{t}} \tag{3.4}$$

The results shown in Fig. 3.28 and Fig. 3.29 correlates well with the expected free jet flow without a fixed boundary layer as it moves from left to right and expands outward and with what has been previously imaged with BOS. The center left of the jet shows the highest intensity of velocity with the flow slowing as it moves to the right and dispersing. Fig. 3.28 shows velocities similar to known values when pixel length is correlated to the known length of the heat gun nozzle.

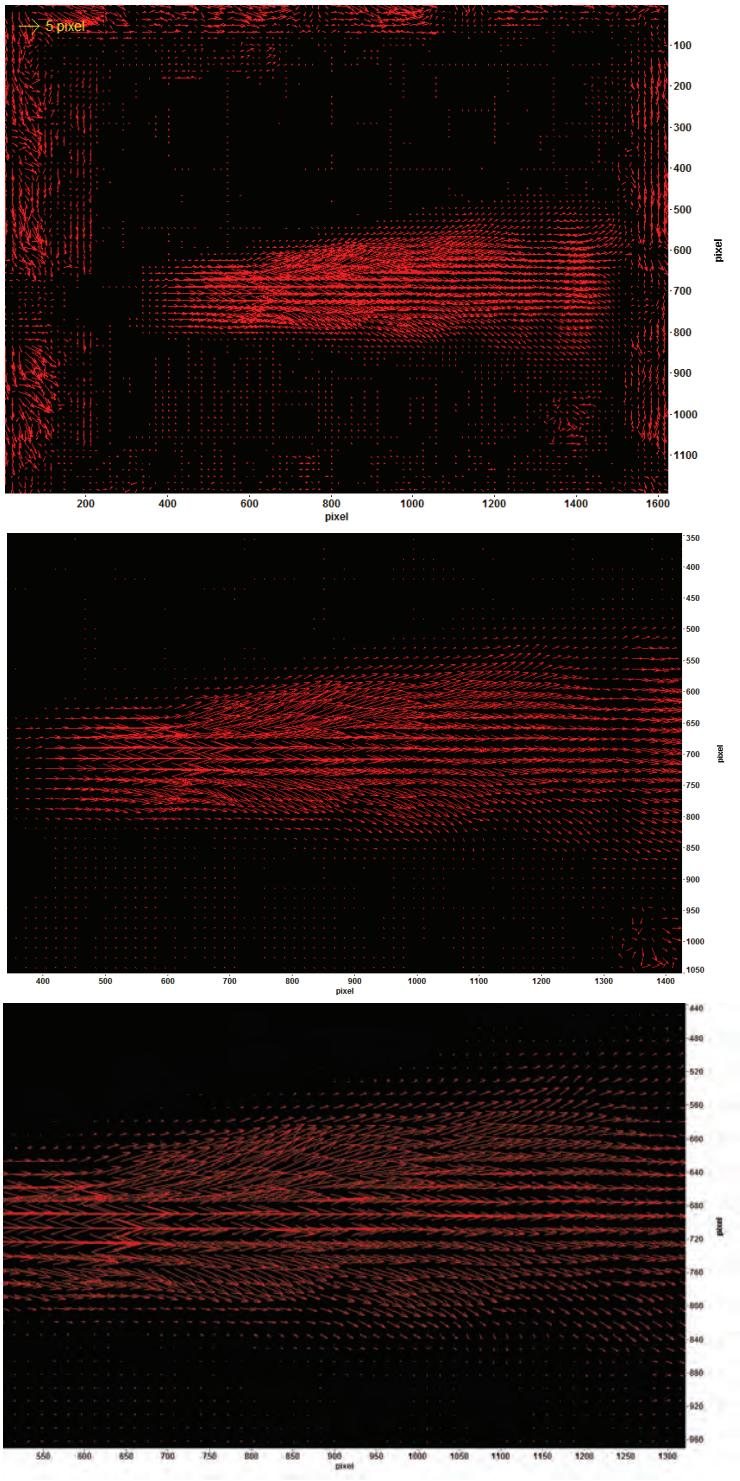

Figure 3.29: Velocity vector map of averaged pixel shift magnitudes of 100 image pairs with increasing flow field magnification

Both of the analysis shown in this section give alternate uses for the BOS flow imaging technique. Beyond the typical qualitative visual imaging shown of BOS testing, there is an inherent ability to extract more data for quantitative analysis. Work in this type of BOS analysis is still in the early stages and will certainly continue to grow as more people use BOS as a flow visualization method.

IV. Conclusions and Recommendations

4.1 Summary of Conclusions

The tests show that size and spacing of the background pattern are the primary attributes for pattern optimization while shape of the pattern does not impact image quality. The dot pattern with 0.05" size and spacing proved to be close to optimization for this setup geometry, and 0.05" was the smallest dot size tested. To truly validate the optimal size, additional tests with smaller dot sizes would have been required for testing to show a lack of improvement in image quality as the size was reduced even further. Testing also revealed that no change in image quality can be discerned by changing background color. Black on white imaged equally well as white on black patterns. Additional testing with high speed video showed the ability of BOS imaging to be used for more than simple qualitative analysis. Quantitative velocity mapping and fine zoom flow analysis can be completed also.

While reviewing the amount of tests taken on each variable, it appears too many tests were focused on comparing the shape variable and more tests could have been taken on the size variable. The shape variable had little to no impact on the imaging results, therefore, it would have been prudent to have done more tests comparing the size variable and less comparing the shape variable. Most literature reviewed used some variation of a dot pattern. It probably would have been sufficient to only do a couple cursory tests for shape comparison to conclusively show and it had no impact. Size and spacing variables appear to be key parameters when developing a background pattern and more tests with size variation could have proven more valuable.

When each of the test series were evaluated for the shape variable in Table 3.3, no discernable variation in image quality could be readily identified. This appeared to be conclusive evidence that the shape of the object in the pattern has little to no bearing on image quality. Since circular dots are easily drawn, they tend to be the shape of choice for most BOS background patterns. Also, the symmetry of dots lends itself well to easily controlling spacing between shapes in the pattern. When non-symmetrical shapes are used they could have a tendency to bunch closely in some locations while leaving larger spacing in other locations. Also, circular shape lends itself well in the software analysis. When the dot shifts position the software calculates that shift in right angles from the surface of the dot. This can be done at any point on the circle, but on a triangle for instance, this can only be done at the three sides.

Overall, this test series seemed to produce consistent results with the current standard practices in the BOS field. The use of small tightly meshed dot patterns with high contrast between dots and backgrounds appear to be sound practice to produce the best image quality results. The PIV software programs used in BOS data processing, such as the DaVis^{TM} program used here, are highly dependent on having large amounts of reference points between images. To achieve these desired large deposits of reference points, it is necessary to mesh dot patterns as closely together as possible while still leaving enough pixels to allow for high contrasts between shape and background. Through previous trial and error, spacing of 2 to 4 pixels between dots is sufficient for the software to delineate the shift occurring between images.

The results of these tests correlate with the previously mentioned preferred pixel dimensions for BOS testing. For this test setup with a 4 foot length to the background and with a subject set at the midway point with a 28mm focal length and 1600 x 1200 resolution, the optimal dot size and spacing was approximately 0.05". Decreasing the spacing below this did not increase image quality and increasing the size above this decreased image quality. This correlates to previous literature of a dot size in the 2 to 4 pixel range. This provides the software ample opportunity to capture the shift in dot location between images. Additional patterns with shapes smaller than 0.05" should have been tested to provide more conclusive recommendations on the lower end of the sizing scale. If the test setup was changed to larger or smaller in scale, it would be a reasonable assumption to plan a background pattern size that correlates to 2 to 4 pixel range.

Additional test setup conditions should have been tested to fully evaluate the 2 to 4 pixel PIV pixel range recommendation over a series of conditions. This thesis only tested optimal sizing on one test geometry. It would have been prudent to test pattern sizing over smaller and larger scale test geometries to better show the correlation between experimental results and PIV particle sizing theory.

Test 26 along with the 3 baseline tests showed no change in image quality with a change in background color. Test 26 had a background with multiple strips of changing background colors. The only change in image quality in this test was the section that had smaller dots with larger spacing. The degradation in image quality correlated with the change in size and spacing, and not with the change in color.

4.2 Recommendations for Future Research

This work creates a starting point for additional research of background improvements in the BOS method. BOS is still in its infancy when compared to imaging techniques such as classical schlieren. For additional background pattern work more in depth testing on exact spacing distances, and analysis of random or pseudo random patterns could be accomplished. Also, a continuation of this work could validate pattern size requirements for larger or smaller test geometries against the 2 to 4 pixel size theory.

Much of the BOS work to date mentions the use of random dot patterns. This is a bit of a misnomer on the part of the authors in my mind. A true random pattern may not be appropriate for BOS, as it may have large regions with no dots and large regions of dots packed on top of each other, depending on the size of the dots and the density of their spacing. If a small enough dot size was used it would mitigate the crowding I mentioned previously, but this of course depends on the test geometry and the size of dot needed. True random patterns could lead to regions where the software would have little to no contrasting reference points for comparison. A pseudo random pattern would be more appropriate for BOS. I would define this pseudo random pattern as a pattern with controlled random variation in it. This could be done by creating small regions of random dots that are repeated, or a full random pattern that is controlled in some method to prevent large amounts of crowding or spacing between shapes. Hargather describes the use of a simple MATLAB® program to create a random pattern using a rand algorithm [5].

Another option for future research in BOS is with the type of background material used. Instead of printing patterns on standard paper or painting on tunnel walls, there are new types of semi-reflective materials such as Scotchlite that appear to have desirable characteristics. These types of materials provide reflection of large amounts of light in some areas along with finely embedded grains. This could provide exceptional contrast of light reflection within very small regions, which would be ideal for BOS.

Finally, analysis of existing raw data in the software tool, such as DaVis^{TM}, could be used for quantitative review. Each pixel shift identified by the software results in a simple delta vector for the light ray passing through the density gradient. Computational analysis of the data inherent in the software analysis of the imaging is possible, and brings the possibility of further characterization the flow.

Bibliography

1. Biss, M. M., K. L. McNesby, J. M. Densmore and B. E. Homan. "Natural-Background-Oriented Schlieren of Full-Scale Explosions". 27th Army Science Conference, Orlando, FL, 2009.

2. Goldhahn, E. and J. Seume. "The Background Oriented Schlieren Technique: Sensitivity, Accuracy, Resolution and Application to a Three-Dimensional Density Field". *Experiments in Fluids*, Exp Fluids(43):241–249, 2007.

3. Hargather, M. J. and G. S. Settles. "Background-Oriented Schlieren Visualization of Heating and Ventilation Flows: HVAC-BOS". 14th International Symposium on Flow Visualization, Daegu, Korea, June 2010.

4. Hargather, M. J. and G. S. Settles. "Recent Developments in Schlieren and Shadowgraphy". volume AIAA 2010-4206. 27th AIAA Aerodynamic Measurement Technology and Ground Testing Conference, Chicago, Illinois, June 2010.

5. Hargather, M. J., M. J. Lawson and G. S. Settles. "Seedless Velocimetry Measurements by Schlieren Image Velocimetry". *American Institute of Aeronautics and Astronautics*, 49(3):611–620, March 2011.

6. Raffel, M., S. Wereley J. Kompenhans, C. Willert. *Particle Image Velocimetry: A Practical Guide*. Springer, 2nd edition, 2007. ISBN 9783540723073.

7. Reinholtz, C. K., K. E. Scott, F. L. Heltsley and M. N. Rhode. "Visualization of Jettison Motor Plumes from an Orion Launch Abort Vehicle Wind Tunnel Model using Background-Oriented Schlieren". volume AIAA 2010-1736. US Air Force Test and Evaluation Days, Nashville TN, February 2010.

8. Richard, H., M. Rein, J. Kompenhans, M. Raffel and G.E.A. Meier. "Demonstration of the Applicability of a Background Oriented Schlieren (BOS) Method". 10th International Symposium on Applications of Laser Techniques to Fluid Mechanics, Lisbon, Australia, 2000.

9. Smith, M. E. "Synthesis of Background Oriented Schlieren from CFD Flow Field". AEDC-ER-10-T-28. Arnold Engineering Development Center, Technology Branch, CFD Group, Arnold AFB TN, 2009. Unpublished Report.

10. Vasudeva, G., D. R. Honnery and J. Soria. "Non-Intrusive Measurement of a Density Field using the Background Oriented Schlieren(BOS) Method". Fourth Australian Conference on Laser Diagnostic in Fluid Mechanics and Combustion, Adelaide, Australia, December 2005.

11. Venkatakrishnan, L. and G. E. A. Meier. "Density Measurements Using the Background Oriented Schlieren Technique". *Experiments in Fluids*, Exp Fluids(37):237–247, 2004.

REPORT DOCUMENTATION PAGE

Form Approved
OMB No. 0704-0188

1. REPORT DATE *(DD-MM-YYYY)*	2. REPORT TYPE	3. DATES COVERED *(From - To)*
14/12/2011	Master's Thesis	Feb 2011 - Dec 2011

4. TITLE AND SUBTITLE
Background-Oriented Schlieren Pattern Optimization

5a. CONTRACT NUMBER

5b. GRANT NUMBER

5c. PROGRAM ELEMENT NUMBER

6. AUTHOR(S)
Hartberger, Jeffery E., Capt, USAF

5d. PROJECT NUMBER

5e. TASK NUMBER

5f. WORK UNIT NUMBER

7. PERFORMING ORGANIZATION NAME(S) AND ADDRESS(ES)
Air Force Institute of Technology
Graduate School of Engineering and Management (AFIT/EN)
2950 Hobson Way
WPAFB OH 45433-7765

8. PERFORMING ORGANIZATION REPORT NUMBER
AFIT/GAE/ENY/11-D16

9. SPONSORING/MONITORING AGENCY NAME(S) AND ADDRESS(ES)
intentionally left blank

10. SPONSOR/MONITOR'S ACRONYM(S)

11. SPONSOR/MONITOR'S REPORT NUMBER(S)

12. DISTRIBUTION/AVAILABILITY STATEMENT
APPROVED FOR PUBLIC RELEASE; DISTRIBUTION UNLIMITED.

13. SUPPLEMENTARY NOTES
This material is declared a work of the U.S. Government and is not subject to copyright protection in the United States.

14. ABSTRACT
This paper describes a test series to investigate background patterns used for the Background-Oriented Schlieren field density measurement technique. Several varying background patterns were substituted under similar fluid density conditions to visualize and isolate the effects of patterns in the background images. A qualitative comparison was completed of the flow visualization results of each background pattern to categorize background conditions that improved the flow visualization image. Changes in background patterns revealed significant changes in flow visualization. Pattern contrast, spacing and sizing all played large parts in the quality of the visual density gradient imaging during the test series.

15. SUBJECT TERMS
Background-Oriented Schlieren, BOS, Background Pattern Optimization, Density Gradient Measurement, Flow Visualization

16. SECURITY CLASSIFICATION OF:			17. LIMITATION OF ABSTRACT	18. NUMBER OF PAGES	19a. NAME OF RESPONSIBLE PERSON
a. REPORT	b. ABSTRACT	c. THIS PAGE			Mark F. Reeder, PhD, USAF (ENY)
					19b. TELEPHONE NUMBER *(Include area code)*
U	U	U	UU	102	(937) 255-3636, x4530 mark.reeder@afit.edu